



iCP version 2.0 – A numerical tool for solving reactive transport in fractured media

Diego Sampietro
Elena Abarca
Jorge Molinero

SVENSK KÄRNBRÄNSLEHANTERING AB

SWEDISH NUCLEAR FUEL
AND WASTE MANAGEMENT CO

Box 3091, SE-169 03 Solna
Phone +46 8 459 84 00
skb.se

ISSN 1402-3091

SKB R-21-09

ID 1921841

October 2022

iCP version 2.0 – A numerical tool for solving reactive transport in fractured media

Diego Sampietro, Elena Abarca, Jorge Molinero
Amphos 21 Consulting S.L.

This report concerns a study which was conducted for Svensk Kärnbränslehantering AB (SKB). The conclusions and viewpoints presented in the report are those of the authors. SKB may draw modified conclusions, based on additional literature sources and/or expert opinions.

This report is published on [www\(skb.se](http://www(skb.se)

© 2022 Svensk Kärnbränslehantering AB

Summary

A common assumption in near-field transport modelling of radioactive waste repositories is to assume homogeneous properties of the engineered barrier systems (EBS), including conservative assumptions of no flow and no diffusive resistance of the waste. However, fractures in cementitious materials or gaps between construction materials to be used in radioactive waste repositories may provide preferential pathways for groundwater ingress and radionuclide escape. A quantitative description of the chemical evolution of these fractured media is needed for a more realistic risk assessment of the repository near-field.

This report presents a reactive transport tool able to handle discrete fracture networks (DFN). The tool is an extension of the interface COMSOL-PHREEQC (iCP) (Nardi et al. 2014) that enables solving reactive transport problems in hybrid systems composed of a reactive porous matrix and reactive discrete fractures. A thorough analysis of the capabilities of COMSOL Multiphysics to solve flow and transport in discrete fractures and in hybrid continuum-discrete systems was needed for the development of this tool. Thus, a set of benchmark problems for flow and transport in fractured systems were solved using COMSOL Multiphysics.

iCP was modified to solve reactive transport problems in pure DFN models and in hybrid models with hydrogeochemical reactions taking place in the fractures. Two benchmark problems were proposed and solved. The results serve to validate the technical developments and show the high potential of iCP as a reactive transport modelling tool to simulate coupled physical and chemical processes.

This report is the first in a series of two reports that describe the development of iCP to handle reactive transport modelling in fractured media. This report focuses on DFN and hybrid models, whereas the second report (Sampietro et al. 2022) focuses on DFN with an extra (spatial) dimension to model porous matrix transport.

Sammanfattning

Vid modellering av närfältet för förvar för radioaktivt avfall är ett vanligt antagande att egenskaperna hos barriärerna är homogena, men förekomst av sprickor i cementbaserade material eller håligheter mellan konstruktionsmaterial i förvaret skulle kunna leda till preferentiella flödes- och transportvägar för radionuklider. För en mer realistisk utvärdering av närfältet krävs därför att den kemiska utvecklingen i sprickiga systemet kan kvantificeras.

Denna rapport presenterar ett beräkningsverktyg för reaktivtransportmodellering som hanterar diskreta spricknätverk (DFN). Beräkningsverktyget är en utveckling av iCP (gränsnitt COMSOL-PHREEQC) (Nardi et al. 2014) och möjliggör reaktiv transportmodellering i hybrid-modeller som består av ett kontinuerligt poröst medium (matris) och diskreta sprickor.

En utförlig analys av förutsättningarna för att lösa flödes- och transportberäkningar i diskreta sprickor och i hybrid-modeller i COMSOL Multiphysics var nödvändig vid modellutvecklingen. Följaktligen användes COMSOL Multiphysics för att beräkna flöde och transport i sprickiga system för några väldefinierade typexempel.

Utvecklingen av iCP syftar till att kunna lösa reaktiv transport i DFN-modeller och i hybrid-modeller i vilka hydrogeokemiska reaktioner sker i sprickorna och det porösa mediumet. Två typexempel av beräkningsproblem presenteras och lösas. Resultaten validerar den utvecklade modellen och indikerar att iCP har en hög potential som reaktivt transportmodelleringsverktyg att simulera kopplade fysiska och kemiska processer.

Denna rapport är den första av två rapporter som beskriver utvecklingen av iCP för reaktiv transportmodellering i sprickiga system. Denna rapport fokuserar på diskreta spricknätverksmodeller (DFN-modeller) och hybridmodeller, medan den andra rapporten (Sampietro et al. 2022) fokuserar på DFN-modeller där matrisen representeras av 1D element (1D matris-metodiken) som möjliggör beräkning av matrisdiffusion.

Contents

1	Introduction	7
1.1	Background	7
1.2	Objectives	8
1.3	Outline of the report	8
2	Modelling of physical and chemical processes in fractured media	9
2.1	Equivalent continuous porous media (ECPM)	10
2.2	Continuous fracture models (CFM) or pure DFN	11
2.3	Discrete fracture-matrix (DFM) or Hybrid models	13
2.4	DFN with an extra dimension	14
2.5	Codes for solving Reactive Transport in fracture media	14
3	Methodology	15
3.1	Code description	15
3.1.1	COMSOL	15
3.1.2	iCP	16
3.2	Governing equations	17
3.2.1	Groundwater flow	17
3.2.2	Conservative transport	18
3.2.3	Physics coupling	19
3.2.4	Chemical reaction modelling	21
4	Results	23
4.1	Groundwater flow	23
4.1.1	Benchmark 1 – Hydrocoin	24
4.1.2	Benchmark 2 – Regular fracture network	26
4.1.3	Benchmark 3 – Complex fracture network	30
4.1.4	Benchmark 4 – Case based on outcrop data	33
4.2	Conservative transport	35
4.2.1	Contaminant transport through a fracture with matrix diffusion	35
4.3	Reactive transport	38
4.3.1	Pure DFN	38
4.3.2	Hybrid method – Reactive fractures and matrix	38
5	Conclusions	49
	References	51

1 Introduction

1.1 Background

Fractures in cementitious materials or gaps between construction materials to be used in radioactive waste repositories are recognised as some of the most significant sources of heterogeneity in the near-field of a repository (Harris et al. 1997). The main risk is that connected fractures act as preferential pathways for groundwater ingress and radionuclide escape. Moreover, fractures and cracks can undergo chemical evolution through mineral precipitation and dissolution that can alter their flow properties increasing the degree of heterogeneity of the system. The quantification of the chemical evolution of fractured media is needed for a more realistic risk assessment of the repository near-field.

The most widely employed approach for reactive transport modelling in the near-field consists of representing fractures and matrix as a continuous porous medium (CPM). However, this approach usually requires a very fine mesh to properly represent the complex geometry of fractures and fracture intersections. Therefore, a greater focus on the development of numerical methods is needed to include and represent accurately the geometry of fracture networks.

A different method to solve transport problems in fracture-matrix systems consists of representing the fractures as a Discrete Fracture Network (DFN). Three different approaches can be identified in dealing with reactive transport modelling in fracture-matrix systems with DFNs. First, the reactive transport in pure DFN models (RTM) which only includes chemical reactions in the discrete fractures. In this approach the thickness of the fracture is neglected. Second, hybrid models in which the fractures are embedded in a porous medium. The fractures are discretized in one dimension less than the porous medium, e.g., fractures are represented as 2D planes in a 3D porous medium. Hybrid models can solve reactive transport in both the fractures and the matrix or assume reactions only in the matrix with fractures acting only as preferential paths for flow and transport. Third, DFN models with an extra dimension, which also solve reactive transport both in fractures and in the matrix. However, in this approach the treatment of the matrix is simplified with respect to the hybrid approach. Thus, instead of a full three-dimensional representation of the matrix, the matrix domain is represented as a set of independent 1D elements connected to the fractures. This extra dimension approach can be applied only when the main mechanism for transport in the matrix is diffusion.

The iCP software platform (Nardi et al. 2014) is an interface developed to simulate reactive transport by coupling the COMSOL Multiphysics and PHREEQC software programs. This Java software provides the communication between the two software programs, and it has proven to be a powerful simulator for complex reactive transport problems (Sainz-Garcia et al. 2017, Karimzadeh et al. 2017). The capability of iCP to simulate groundwater flow and reactive transport in porous media has been extensively tested. However, previously iCP was not able to solve reactive transport in fractured media.

In addition to the technical challenges, there are still conceptual challenges in modelling reactive transport in discrete fractures. A key point is related to the conceptualization of the matrix-fracture interface. Most transport codes assume concentration continuity between the matrix and the fractures. This means that fracture and matrix cannot be treated as separate geochemical domains. Thus, the continuity assumption neglects the variability of fracture properties (aperture, permeability, porosity) induced by geochemical reactions occurring independently of the processes in the matrix. To overcome this limitation, separate geochemical domains are required for the matrix and fractures.

This report presents an extension of iCP (Nardi et al. 2014) to simulate reactive transport in fractured media. In particular, iCP has been modified to solve reactive transport problems with hybrid models composed of a reactive porous matrix and reactive discrete fractures. A thorough analysis of the capabilities of COMSOL Multiphysics to solve flow and transport in discrete fractures and in hybrid (continuum-discrete) system is needed for the development of this tool. Therefore, a set of benchmark problems for flow and transport in fractured systems have been solved with COMSOL Multiphysics.

1.2 Objectives

The main objective of this work is to develop and present a new version of iCP to solve reactive transport in DFN models and to verify its applicability in the near-field.

In addition, this report provides benchmarking exercises to validate the processes implemented in the reactive transport models such as groundwater flow in fractures, conservative transport in fractures with/without matrix and conservative transport in fractures with the matrix implemented as an extra dimension (which is discussed in more detail in a second report by Sampietro et al. (2022) in this series of two reports on the development of iCP to handle reactive transport modelling in fractured media).

1.3 Outline of the report

This report consists of five chapters. Chapter 1 provides introduction to the study with the key motivation and objectives. Chapter 2 contains a thorough review of the state of the art of reactive transport modelling in fracture media describing the numerical methods and available tools. Chapter 3 describes the step-wise methodology for the development and benchmarking of the new version of iCP that handles reactive transport in DFN models. This chapter also details the tools and governing equations used in iCP for DFN. The numerical results of the benchmarking tests carried out to validate the developed software are presented in Chapter 4. Chapter 5 summarizes the main outcomes of the work.

2 Modelling of physical and chemical processes in fractured media

Heterogeneity can play an important role in groundwater flow and solute transport in the near-field of a repository. A common source of heterogeneity is the presence of fractures, which dominate hydrological, geochemical and geomechanical behaviour of materials (Lei et al. 2017). Berkowitz (2002) distinguished between two types of fractured media: fractured media and fractured porous media. The concept of fractured media emphasises the fractures themselves, whereas the concept fractured porous media also includes the effect of the porous media on the modelled process. The impact of the presence of fractures on different physical processes such as groundwater flow, contaminant transport and slope stability has motivated the development of different approaches to include these heterogeneities in numerical methods.

A good review of conceptual methods to represent fractures in numerical models can be found in Flemisch et al. (2018) and in Berkowitz (2002). In these papers, the authors discuss several conceptual and numerical approaches to simulate physical processes in fractured media. They refer, among others, to the methods proposed in Dietrich et al. (2005), Hoteit and Firoozabadi (2008), Neuman (2005), Sahimi (2011) and Singhal and Gupta (2010).

Conceptually, the simplest approach to model flow and transport in fracture-matrix systems is to consider both the fractures and matrix as a continuous porous medium (CPM). In CPM models, fractures can be treated as a continuous porous medium with homogeneous properties or, alternatively, fractures can be treated as an equivalent continuous porous medium (ECPM) with upscaled flow and transport properties based on a specific DFN, see Figure 2-1C.

A different approach to describe flow and transport of contaminants in fractured media consists of representing the fractures as discrete structures (DFN). Particularly, in the context of modelling reactive transport problems, different approaches can be identified and classified in three broad categories. First, the pure DFN, also termed Continuous Fracture Models (CFM) in Flemisch et al. (2018), that only includes chemical reactions in the fractures and neglects the fracture-matrix interactions in the modelled processes, see Figure 2-1A. Second, hybrid models, also termed Discrete Fracture-Matrix models (DFM), in which fractures are discretized in one dimension less than the porous medium. For example, in Figure 2-1B, fractures represented as 2D planes are embedded in a 3D porous medium. Hybrid models can handle chemical reactions in both the fractures and the matrix or, alternatively, a reactive matrix with non-reactive fractures. Third, DFN models with an extra dimension, which solve reactive transport in the fractures and the matrix, but the matrix is treated as an additional spatial dimension.

The following subchapters describe these different numerical models and available tools to solve reactive transport problems in fracture media.

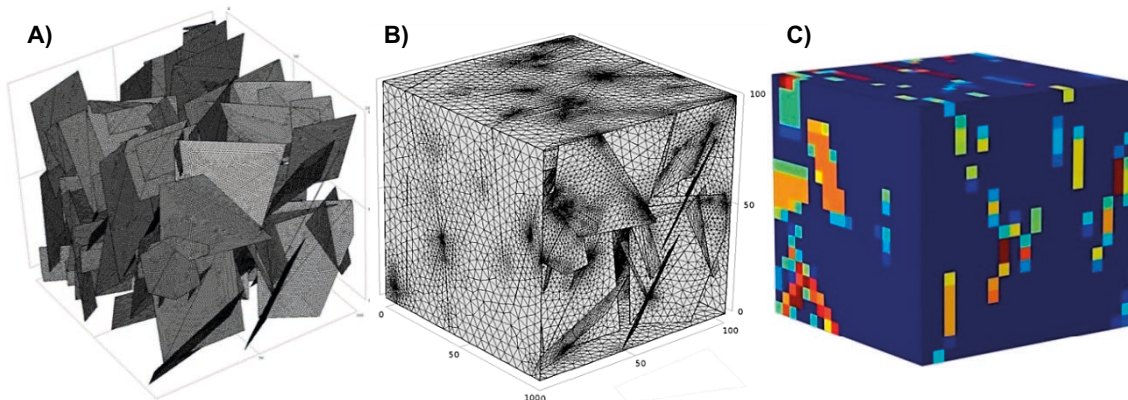


Figure 2-1. A) Finite-element mesh formed by triangles used to solve the groundwater flow in a DFN model, B) Finite-element mesh formed by tetrahedra and triangles used to solve the groundwater flow in a hybrid model. C) Equivalent continuous porous media model used to solve the groundwater flow.

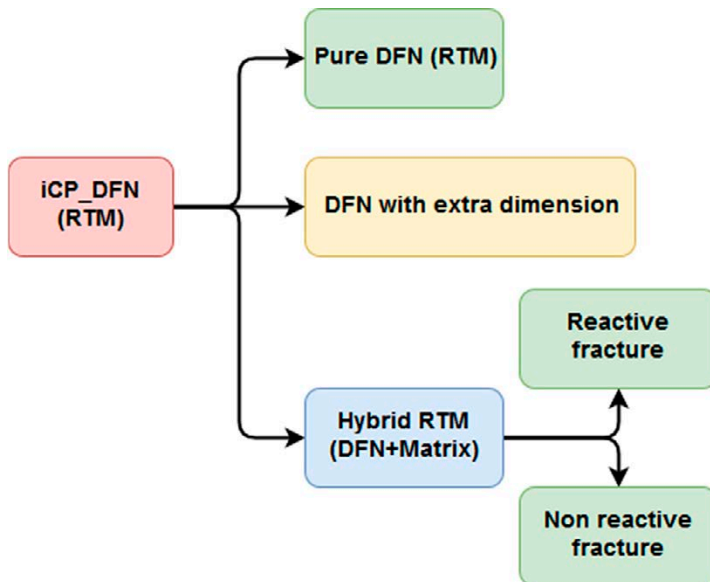


Figure 2-2. Different approaches to model reactive transport in fractures.

2.1 Equivalent continuous porous media (ECPM)

In ECPM models, the fractured medium is represented by a heterogeneous and anisotropic continuous porous medium, see Figure 2-1C. The heterogeneity and anisotropy are introduced in a CPM model in order to represent the underlying DFN. Therefore, in order to set up ECPM models, generated DFN models are required. After applying upscaling methods, the fracture properties in ECPM models are equivalent in terms of the averaged properties or resistance to flow and transport fluxes to the underlying DFN.

ECPM models are computationally feasible for large or regional-scale applications. However, ECPM models require upscaling of DFN into ECPM that will condition the flow and transport results. Methods to upscale hydraulic properties have been well studied and tested. There are two main methods used to upscale hydraulic parameters. One method is the geometric upscaling, which is implemented in the code DarcyTools (Svensson and Ferry 2010). This method consists of computing the hydraulic conductivity of the cell as a function of the volume of the fractures intersecting the cell volume (Svensson 2001). Thus, the geometric upscaling method ensures the consistency of the geometry. The second method is the hydraulic upscaling (Jackson et al. 2000), which is included in the software programs ConnectFlow (Jacobs 2021). This method consists of estimating an equivalent hydraulic conductivity of the cell such that the flow crossing the cell volume is the same as the one crossing the fracture in the DFN model. Therefore, the hydraulic upscaling method preserves the mass balance per cell volume (Jackson et al. 2000). The hydraulic upscaling provides a full tensor of the hydraulic properties in all directions. Also, dead-end fractures are better handled with the hydraulic upscaling.

The upscaling of transport parameters involves obtaining equivalent parameter values for porosity, dispersivities and effective diffusivities. Nowadays, much effort is being dedicated to proposing methods for the upscaling of transport properties and improving the accuracy of the ECPM method to simulate the transport of dissolved species (Baxter et al. 2019). However, the applicability of these upscaling methods to commercial software is still in developmental stages. Methodologies to upscale the porosity geometrically are presented in Svensson (2001), Svensson and Ferry (2010), Jacobs (2021) and Baxter et al. (2019).

The generation of heterogeneous property fields is implemented in different software such as SGeMS (Remy et al. 2009), which is a geostatistical software that can generate heterogeneous domains, and ConnectFlow (Jacobs 2021) and DarcyTools (Svensson and Ferry 2010). Codes that cannot generate ECPM but can perform simulations using existing ECPM are Modflow (Harbaugh 2005), Feflow (Diersch 2013), and COMSOL Multiphysics (COMSOL 2017), etc.

Recently, an upscaling methodology has been implemented in the COMSOL Application to evaluate the directional equivalent permeability of the fractures according to the methodology proposed by Renard and de Marsily (1997) and Jackson et al. (2000). Figure 2-3 shows upscaled permeability fields (for different mesh discretization) for a specific DFN realization with 250 fractures.

2.2 Continuous fracture models (CFM) or pure DFN

CFM or pure DFN models describe processes occurring only in fractures and neglect the interaction between fractures and the matrix (Figure 2-1A). This approach is adequate for simulating the fluid movement in crystalline rocks or other materials where the permeability of the fractures is several orders of magnitude larger than the one in the matrix. However, for solute transport, diffusion through low permeability matrix can be a critical process (Grisak and Pickens 1980, Neretnieks 1980). Therefore, this approach is not valid when advection, diffusion or dispersion in the matrix are non-negligible.

Specifically, the method consists of representing the fractures as surfaces in 3D models or as lines in 2D models. There are different methods to include matrix diffusion in CFM without including the whole matrix domain in the model. These methods are detailed in Section 2.4 dedicated to explaining different approaches to model matrix diffusion.

CFM or pure DFN models generate more realistic and accurate groundwater flow fields than the one obtained using an ECPM approach (Jackson et al. 2000).

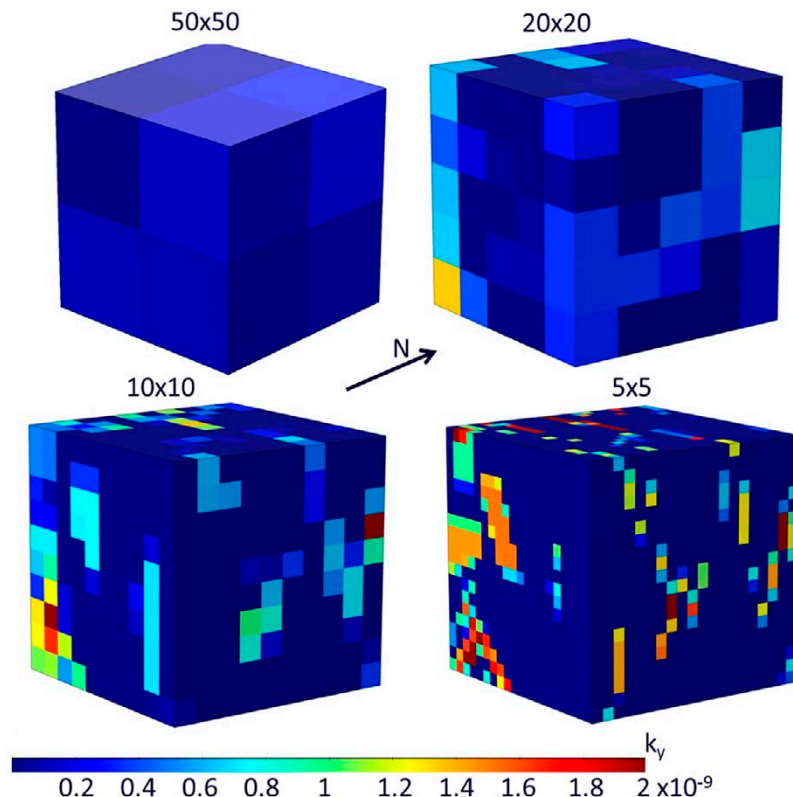


Figure 2-3. Permeability fields obtained using the upscaling method by Renard and de Marsily (1997) on a DFN realization with 250 fractures. Permeability fields for different mesh discretization are shown (pixel a pixel sizes are given in the figure).

CFM modelling can be performed with different commercial and open source software such as DFNworks (Hyman et al. 2015), NAPSAC, which now is available within Connectflow software (Hartley et al. 1996, Jacobs 2021) and Fracman (Ford et al. 2008). These software programs can be used to perform solute transport simulations, although the influence of the matrix on the transport is not considered in most of them. An example of contaminant transport modelling using this method can be found in Hadgu et al. (2017). However, aforementioned codes except Connectflow (Jacobs 2021) do not simulate reactive transport problems.

The main benefit of the CFM models is the possibility of excluding the low permeable matrix from the numerical model, which reduces the needed computational resources, and a better discretization in the fractures. A disadvantage of this approach is that it neglects processes such as the seepage from the low permeable matrix. In addition, in the case of regional modelling, with tens of thousands fractures, this method becomes inefficient compared to ECPM approach due to the high computational resources needed (Jackson et al. 2000, Jacobs 2021). Thus, application of CFM models to large or regional-scale problems fails due to the complex geometrical representation of the fractures (Lei et al. 2017), which usually implies the generation of very refined meshes with a large number of elements.

Since version 5.1, the software program COMSOL Multiphysics allows to read and import a DFN geometry and hydraulic properties from a .fab file. The software builds the DFN and creates the finite element mesh. To validate this feature in COMSOL, three DFN models with 250, 3 000 and 30 000 fractures were generated, see Figure 2-4. The validation was carried out by solving groundwater flow with the fracture flow physics interface in COMSOL. The results of the flow simulations with 250 and 3 000 fractures were compared successfully against the results from other software programs such as DarcyTools (Svensson and Ferry 2010), which solves flow in an upscaled medium, and FracMan (Ford et al. 2008). This comparison demonstrated a high potential of COMSOL to handle DFN modelling without the need of using an upscaled field.

Regarding reactive transport, CFM or pure DFN models as discussed for the transport of aqueous species consider only chemical reactions in the fractures without any diffusion or reactions in the matrix.

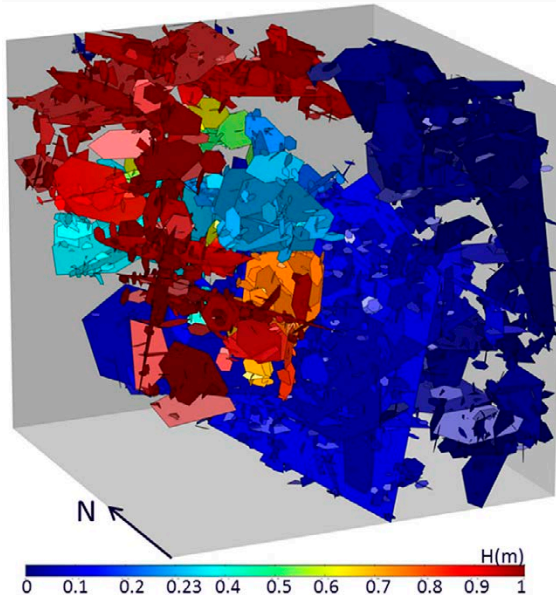


Figure 2-4. Solution of a benchmark problem using a COMSOL DFN of 3 000 fractures. The surfaces of the fractures are coloured according to the calculated groundwater head.

2.3 Discrete fracture-matrix (DFM) or Hybrid models

The DFM or hybrid models (Figure 2-1B) consider flow occurring in the fracture network and in the surrounding porous media. These models are appropriate to use when the effect of the porous media is important for the processes modelled.

There are different discretization methods that solve DFM models. One of the most efficient ways to represent fractures in this method is the hybrid-dimensional approach (Helmig 1997, Monteagudo and Firoozabadi 2004, Karim-Fard et al. 2004, Martin et al. 2005, Reichenberger et al. 2006, Flemisch et al. 2018) where fractures are discretized as elements of co-dimension one with respect to the surrounding matrix dimension. This is the method that most of the codes use to model groundwater flow in DFN. Non-conforming DFM models have been developed in recent years, such as EDFM (Moinfar et al. 2011, Hajibeygi et al. 2011), XFEM-based approaches (D'Angelo and Scotti 2012, Schwenck 2015, Huang et al. 2011), or mortar-type methods (Frih et al. 2012). A summary of the main features of the methods cited above is detailed in Table 2-1. The methods in the table refer to the applied numerical approach according to the terminology in Flemisch et al. (2018). The fracture dimension distinguishes the dimension of the fracture compared to the dimension of the porous media (e.g. dim-1 refers to a numerical method where the fracture has one dimension less than the porous media) and conforming refers to the properties of the mesh. Thus, the elements of the mesh are conforming if their edges and faces match exactly, and non-conforming otherwise. This applies to the geometry, the properties of the medium or both. Finally, pressure continuity refers to the existence of continuity or discontinuity in the fluid pressure between the fractures and the adjacent matrix.

In addition to the above-mentioned methods, there are other numerical methodologies that uses a hybrid approach like those reported in Nick and Matthäi (2011), Bazrafkan et al. (2014), Milliotte et al. (2018) and Odsæter et al. (2019). Regarding solute transport, DFM models allow to model the transport of diluted species by accounting for advection, diffusion and dispersion in both the porous and fracture domains. The most relevant feature of these models is that fractures are represented as lower-dimensional objects within the porous matrix.

In hybrid models continuity of the dependent variables (pressure, concentration, etc) can be assumed across the fracture-matrix interface. If continuity is assumed, the dependent variable is assumed to be the same in both domains. The hybrid models which allow discontinuity in the dependent variables, assume mass conservation between the matrix and the fracture. Then, an exchange term between the fractures and matrix is defined. The meaning of this exchange term is discussed in more detail in Section 3.2.3.

Most of the existing numerical codes and software programs that solve reactive transport models using a DFM approach assume continuity between the matrix and the fracture. Therefore, the concentration of the different species in the fracture and matrix is forced to be equal in the nodes of the mesh that form part of both fracture and matrix. The present work explores both approaches: continuity and non-continuity of dependent variables.

Table 2-1. Different DFM discretization methods for solving groundwater flow reported in Flemisch et al. (2018).

Method	Fracture dimension	Conforming	Pressure continuity
Box-DFM	dim-1	yes	yes
CC-DFM	dim-1	yes	no
EDFM	dim-1	no	yes
mortar-DFM	dim-1	geometrically	no
P-XFEM	dim-1	no	no
D-XFEM	dim-1	no	no
MFD	dim	geometrically	no

DFM models are more realistic than CFM models because they include the effect of the matrix. However, their main disadvantage is the computational cost induced by the requirement of complex meshes.

The DFM method has been implemented in several commercial modelling software programs such as COMSOL Multiphysics (COMSOL 2017), Feflow (Diersch 2013), Transin (Carrera et al. 1995).

Hybrid models of reactive transport can be divided into two categories depending on whether the fracture is considered a reactive domain or not (Figure 2-2). From a conceptual point of view, a fracture can be seen merely as a preferential flow path for groundwater and dissolved species. However, solute transport in the fractures can promote reactions between the minerals and the groundwater. Mineral precipitation/dissolution processes in the fractures might modify the fracture aperture and therefore impact on the hydraulic behaviour of the groundwater and the solute transport. Therefore, the hybrid models that include reactivity in both fractures and matrix should include independent geochemical domains for the fractures and matrix and discontinuity in the concentrations. In this case, the concentrations in the fracture and matrix are coupled via a mass transfer term. This approach has been implemented in iCP (Nardi et al. 2014). This hybrid method requires meshing the fracture and the matrix domains which implies a considerable computational cost. However, this is the most integrated approach.

2.4 DFN with an extra dimension

The extra dimension approach includes the fractures and the matrix, the latter represented as an additional spatial dimension. These models are adequate when the permeability of the matrix is very low and transport in the matrix is diffusion dominated. In the extra dimension models the matrix diffusion of dissolved species is considered by using analytical or numerical approaches, e.g., matrix diffusion (Carrera et al. 1998), continuous time random walk (Painter and Cvetkovic 2005, Dentz and Berkowitz 2003, Berkowitz and Scher 1997, 1998), multi-rate mass transfer (Haggerty and Gorelik 1995, Hollenbeck et al. 1999). These methods allow for inclusion of reacting terms that affect the chemical composition of the fluid in the fracture, considering properties of both the surrounding matrix and the fracture. The effect of the matrix diffusion is included without meshing the matrix domain in a similar way defined in the Dual Continuum models proposed by Iraola et al. (2019) or the rock matrix diffusion method detailed in Jacobs (2021). In extra dimension models, the fractures and the matrix are coupled via a mass exchange term, and matrix diffusion parallel to the fractures is neglected. The implementation of DFN with an extra dimension in iCP is covered by a second report in this series of two reports on the development of iCP to handle reactive transport modelling in fractured media.

2.5 Codes for solving Reactive Transport in fracture media

The concepts for describing groundwater flow and transport discussed above, i.e., CPM, DFM and ECPM, can also be used for solving reactive transport problems. Although, there are several codes that can solve the groundwater flow and the conservative transport in fractured porous media, only a few can handle chemical reactions. Software programs with this capability are ConnectFlow (Jacobs 2021), Pflotran (Hammond et al. 2007) and Feflow (Diersch 2013). Pflotran solve reactive transport problems using an ECPM approach to represent fractures. Feflow uses a DFM approach assuming continuity between fractures and matrix. Thus, this approach does not allow to simulate processes such as clogging or dissolution in fractures (Diersch 2013). Connectflow (Applegate et al. 2020, Jacobs 2021) can handle different approaches such as ECPM, CPM or DFN with extra dimension (rock matrix diffusion in Jacobs (2021)).

In addition to the above-mentioned codes, there are several software programs to solve flow and reactive transport in porous media available. PHREEQC (Parkhurst and Appelo 2013) and HP1 (Šimůnek et al. 2006) for 1D applications, or PHAST (Parkhurst et al. 2004), PHT3D (Prommer et al. 1999), CRUNCHFLOW (Steefel and MacQuarrie 1996), and RETRASO (Saaltink et al. 1997). However, their applicability is still relatively limited due to the lack of either flexibility to integrate new physics or user-friendly interfaces (Nardi et al. 2014). All these software programs can handle flow and transport properties for heterogenous media (e.g. an ECPM), although the DFN upscaling algorithm necessary to obtain the ECPM model is not included. An additional approach to solve reactive transport problems in fractured porous media is to conceptualize a fracture as a discrete porous domain of the same dimension as the matrix. However, this method requires to mesh the fractures which are usually characterized for having a very narrow aperture compared with its extent in the longitudinal and transverse direction. Because of this the approach has a high computational cost for practical use. An example of this approach can be found in Sidborn et al. (2014).

3 Methodology

Different benchmarking exercises used to test and validate the capability of the new version of iCP to solve reactive transport in DFN, are presented below:

- Groundwater flow tests

First, four different Benchmark problems proposed by Flemisch et al. (2018) have been reproduced with COMSOL to validate the implementation of fractures.

- The first test is based on the international Hydrocoin project (OECD 1987). This problem considers a 2D vertical cross-section with two high conductive fractures that intersect a crystalline matrix.
- The second benchmark is based on Geiger et al. (2013) with a slightly modified boundary condition. The model setup includes a fracture network and a matrix domain.
- The third benchmark represents a set of fractures with different permeability in a matrix domain of 1×1 m.
- The last flow benchmark considers a case based on data from an outcrop located in Norway.

- Conservative transport

A simple conservative transport problem in a fracture-matrix system is used to test the implementation of non-reactive transport in fractures in COMSOL Multiphysics. This problem has previously been used to test codes such as Pflotran (Hammond and Lichtner 2010) and PHAST (Parkhurst et al. 2004). Numerical results are compared with the analytical solution proposed by Tang et al. (1981) for the transport of a tracer through a fracture affected by matrix diffusion.

- Reactive transport

Two different benchmark problems are used to validate the capability of the new version of iCP to solve reactive transport in DFN and in hybrid models and verify its applicability in the near-field. The first validation model is based on example 3 “Cation Exchange” in the iCP User’s Guide (Nardi et al. 2020). This example is based on example 11 in the PHREEQC User’s Guide (Parkhurst and Appelo 2013) and has been widely used as a benchmark problem (e.g. Kolditz et al. 2012). The second validation model is based on the problem presented by Martinez-Landa et al. (2012). The problem considers a two-dimensional synthetic model of a crystalline rock where the groundwater flow is controlled by fractures. Mixing between the natural granitic water and the water leached from concrete leads to precipitation of calcite.

3.1 Code description

3.1.1 COMSOL

COMSOL Multiphysics is a powerful finite element software for the modelling and simulation of physics-based systems based on partial differential equations (PDE) and/or ordinary differential and algebraic equations (COMSOL 2017). The main advantage over other codes is its ability to account for coupled multi-physics phenomena in a flexible way. The software furthermore offers interfaces to CAD software, technical computing software, and script programming in Java. In this work, the subsurface flow module (COMSOL 2017) has been used in addition to the base software package.

The subsurface flow module includes predefined equations and boundary conditions to simulate the groundwater flow in porous media (Darcy’s law) and the transport of diluted species in porous media. The present version of COMSOL (COMSOL 5.3) includes support to solve the equations governing the groundwater flow and transport in fractures (“fracture flow” and “transport of diluted species in fractures”, respectively). These two features allow modelling of discrete fracture networks using a continuous fracture model (CFM) approach. In addition, COMSOL version 5.3 includes a feature in “Darcy’s law” and “transport of diluted species in porous media” physics interfaces called “fracture” that allows simulation of the groundwater flow and transport of diluted species in DFN

using the hybrid approach. It is a Continuous Fracture matrix Model (CFM). This new feature allows solving fully coupled processes in the porous and fractured domains. This methodology assumes continuity in pressure at the fracture-matrix interface.

3.1.2 iCP

The interface COMSOL-PHREEQC (iCP) (Nardi et al. 2014) is used for the mechanistic reactive transport simulations. iCP is an interface that couples COMSOL Multiphysics (COMSOL 2017) and the geochemical simulator PHREEQC (Charlton and Parkhurst 2011). This interface allows for the solution of a wide range of multiphysics and chemical problems and has been successfully used to model complex natural and engineered environments (Sáinz-García et al. 2017, Karimzadeh et al. 2017). iCP is written in Java and uses the IPHREEQC++ dynamic library and the COMSOL Java API. Furthermore, it takes advantage of the multicore computer architecture by balancing the computational load over different threads. iCP is a commercial software distributed by Amphos 21 (<https://techlabs.amphos21.com/technology/interface-COMSOL-phreeqc/>). The current version 2.0 works with all COMSOL versions available in the market and uses the most updated IPhreeqc library. Figure 3-1 shows the flow of information between iCP, COMSOL and PHREEQC.

The reactive transport problem is highly nonlinear (Steefel et al. 2005) and it is commonly solved using an operator-splitting (OS) approach, where solute transport and geochemical reactions are evaluated separately (Strang 1968). iCP is based on implementing an OS technique for solving the flow and transport problem in COMSOL and the chemical system of algebraic and differential equations in PHREEQC. In iCP, physics and reactions are separated using a sequential non-iterative approach (SNIA). If compared with the sequential iterative approach (SIA) scheme, the SNIA does not pose global convergence problems although a tight control on the time step is required to minimize splitting errors (Barry et al. 1996).

A chemical component is defined as a linear combination of species whose mass is not affected by equilibrium reactions (Smith and Missen 1982, Saaltink et al. 1998). It is important to notice that PHREEQC solves the equation over component concentrations but also the necessary equations to solve the species concentrations and the reaction rate terms associated with equilibrium and kinetic reactions, respectively. From the calculated mineral concentrations, the interface updates the porosity, which is returned to COMSOL for the next time step calculation.

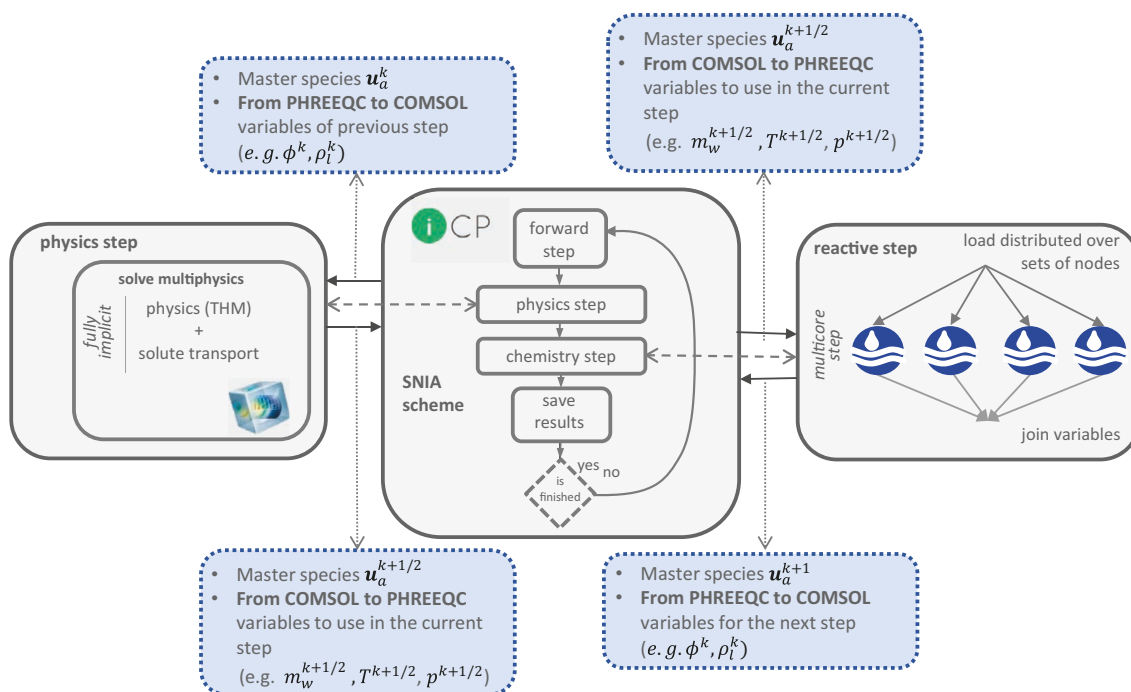


Figure 3-1. Main structure and workflow chart of iCP (Nardi et al. 2020). Information transfers from PHREEQC to COMSOL and from COMSOL to PHREEQC are shown.

In this work, a new version of iCP was developed. This version works for hybrid models that include discrete fractures and a porous matrix. Transport can be solved using the COMSOL physics interfaces “transport of diluted species in porous media” and “transport of diluted species in fractures”. The use of the two transport equations allows solute concentrations to be calculated in fractures and ambient matrix. The expression used to prescribe the mass fluxes connecting the transport of aqueous species in the porous matrix with the transport in fractures is discussed in detail in Section 3.2.3.

A new iCP-related physics interface (“fracture PHREEQC results”) has been implemented in COMSOL to store the results of the chemical system in the fracture domains. After these improvements, iCP can solve reactive transport problems in discrete fractures following the approaches in Figure 2-2.

3.2 Governing equations

3.2.1 Groundwater flow

Groundwater flow in porous media

Flow in porous media is described by combining Darcy's law (Darcy 1856) with the continuity equation and an equation of state for the pore fluid (Bear 1972). Darcy's law is a phenomenological law that relates the specific discharge, or the Darcy velocity, to the hydraulic gradient and the hydraulic conductivity.

Darcy's law states that the fluid velocity is related to the pressure gradient, fluid viscosity and the porous medium properties. The equation can be written as:

$$\vec{u} = -\frac{\vec{k}}{\mu}(\vec{\nabla}p + \rho g \vec{\nabla}z), \quad (3-1)$$

where \vec{u} ($m^3_{\text{water}}/m^2_{\text{surface}}/s$) is the Darcy velocity or the specific discharge vector, \vec{k} (m^2) is the permeability of the porous medium, μ (Pa·s) is the fluid dynamic viscosity, p (Pa) is the fluid pressure, ρ (kg/m^3) is the fluid density, g (m/s^2) is the gravitational acceleration constant and z (m) refers to the elevation.

The continuity equation for saturated flow in a porous medium is:

$$\frac{\partial(\rho\phi)}{\partial t} + \vec{\nabla} \cdot (\rho\vec{u}) = Q_m, \quad (3-2)$$

where, ϕ ($m^3_{\text{pores}}/m^3_{\text{medium}}$) is the porosity and Q_m ($kg/m^3/s$) is a mass source term. By combining Equations (3-1) and (3-2), we obtain the generalized governing equation for fluid pressure:

$$\frac{\partial(\rho\phi)}{\partial t} + \vec{\nabla} \cdot \left[-\frac{\vec{k}\rho}{\mu}(\vec{\nabla}p + \rho g \vec{\nabla}z) \right] = Q_m \quad (3-3)$$

The time derivative can be expanded. By defining porosity and density as functions of pressure and applying the chain rule, the first term in Equation (3-3) can be written as:

$$\frac{\phi\partial\rho}{\partial t} + \frac{\rho\partial\phi}{\partial t} = \phi \frac{\partial\rho}{\partial p} \frac{\partial p}{\partial t} + \rho \frac{\partial\phi}{\partial p} \frac{\partial p}{\partial t}, \quad (3-4)$$

where the first term is due to compressibility of the fluid in the pores and the second is due to compressibility of the bulk aquifer material. By inserting the definition of fluid compressibility ($X_f = (1/\rho)(\partial\rho/\partial p)$) and rearranging, the generalized equation takes the form

$$\rho S \frac{\partial p}{\partial t} + \vec{\nabla} \cdot \left[-\frac{\vec{k}\rho}{\mu}(\vec{\nabla}p + \rho g \vec{\nabla}z) \right] = Q_m, \quad (3-5)$$

where S (1/Pa) is the storage coefficient, which includes contributions due to compressibility of the bulk aquifer material and the fluid in the pores.

Groundwater flow through discrete fractures

The equation solved in the discrete fractures is a modification of Equation (3-1). This equation is based on a tangential version of the Darcy's law, i.e., the flow is driven by the gradient restricted to the tangential plane of the fracture, ∇_T ,

$$\vec{u}_f = -\frac{\vec{k}_f}{\mu} d_f (\vec{\nabla}_T p + \rho g \vec{\nabla}_T z), \quad (3-6)$$

where u_f ($\text{m}^3/\text{m}_{\text{fracture}}/\text{s}$) is the volume flow rate per unit length of fracture, k_f (m^2) is the fracture permeability, d_f (m) is the aperture of the fracture. The mean Darcian fluid velocity within fracture is $v_f = u_f/d_f$. The gradient operator is split into two components, one normal and one tangential to the fracture surface. As an example, the gradient of p can be written as

$$\vec{\nabla} p = \vec{\nabla}_n p + \vec{\nabla}_T p, \quad (3-7)$$

where $\vec{\nabla}_n = \hat{n}(\hat{n} \cdot \vec{\nabla})$ is the normal component, $\vec{\nabla}_T = \vec{\nabla} - \vec{\nabla}_n$ is the tangential component and \hat{n} is a unit length vector normal to the fracture surface. The normal gradient is defined in the direction normal to the boundary representing the fracture and the tangential gradient is defined along the boundary. Here, the normal gradient is assumed to be negligibly small in comparison to the tangential and therefore:

$$\vec{\nabla} p \approx \vec{\nabla}_T p. \quad (3-8)$$

A single equation for the pressure can be obtained by combining Equation (3-6) with the continuity equation. To restrict the continuity equation to the tangential plane of the fracture, the equation is integrated over the fracture aperture. This gives:

$$d_f \frac{\partial}{\partial t} (\phi_f \rho) + \vec{\nabla}_T \cdot (\rho \vec{u}_f) = d_f Q_f, \quad (3-9)$$

where ϕ_f ($\text{m}^3_{\text{pores}}/\text{m}^3_{\text{medium}}$) is the fracture porosity, Q_f ($\text{kg}/\text{m}^3/\text{s}$) is the mass source term. In the case of fractures, it is common to speak in terms of transmissivity, T_f (m^2/s). This is the integral of the hydraulic conductivity over the thickness of the fracture. For a fracture with constant hydraulic conductivity K (m/s), we obtain:

$$\vec{T}_f = \vec{K} \cdot d_f \quad (3-10)$$

3.2.2 Conservative transport

Transport of diluted species in porous media

The transport of solutes in a variably saturated porous medium is described through the advection-diffusion/dispersion equation (ADE) (Bear 1972):

$$(\phi \rho_l) \frac{\partial c_i}{\partial t} + \rho_l \vec{u} \cdot \vec{\nabla} c_i = \rho_l \vec{\nabla} \cdot [(\vec{D}_D + \vec{I} D_e) \cdot \vec{\nabla} c_i] + \rho_l \phi r_{eq} + \rho_l \phi r_{kin} \quad (3-11)$$

where c_i (mol/kg_w) is the concentration of species i in solution, u (m/s) is the Darcy velocity field, ϕ (m^3/m^3) is the porosity of the rock, ρ_l (kg/m^3) is the fluid density, D_D (m^2/s) is the dispersion tensor, which depends on the longitudinal and transverse dispersivities, I is the identity matrix and D_e (m^2/s) is the effective diffusivity in the liquid phase. r_{eq} and r_{kin} (mol/kg_w) refer to reactive rate vector related to equilibrium and kinetic reactions, respectively. The Darcy velocity field is calculated based on the groundwater flow Equation (3-1). For an isotropic porous medium, the dispersion tensor depends on the longitudinal (α_L) and transverse dispersivity (α_T) (m). In a Cartesian coordinate system, the dispersion tensor can be written as:

$$(\vec{D}_D)_{mn} = \alpha_T |\vec{u}| \delta_{mn} + (\alpha_L - \alpha_T) \frac{u_m u_n}{|\vec{u}|} \quad (3-12)$$

where δ_{mn} is the Kronecker delta, $m, n \in \{x, y, z\}$ and u_m is the m :th component of the Darcy velocity field. Dispersivity is a scale-dependent parameter (Gelhar et al. 1992) and, in heterogeneous media, it depends on the correlation scale of heterogeneities (Gelhar and Axness 1983).

Transport of diluted species in fractures

The equation to solve the mass transport of a species c_i in a fracture embedded in a porous medium is:

$$d_f \left[(\phi \rho_l) \frac{\partial c_i}{\partial t} + \rho_l \vec{\nabla}_T \cdot ((\vec{D}_D + \vec{D}_e) \vec{\nabla}_T c_i) + \rho_l \vec{u} \cdot \vec{\nabla}_T c_i \right] = n_o + d_f \rho_l \phi r_{eq} + d_f \rho_l \phi r_{kin} \quad (3-13)$$

where d_f (m) is the fracture thickness, $\vec{\nabla}_T$ is the gradient tangential to the fracture surface and n_o ($\text{mol}/\text{m}^2/\text{s}$) corresponds to out-of-plane flux from the neighbouring porous domain. The normal gradient is assumed to be negligibly small in comparison to the tangential and therefore:

$$\vec{\nabla} c_i \approx \vec{\nabla}_T c_i \quad (3-14)$$

3.2.3 Physics coupling

Groundwater flow coupling

The models presented here consider the coupling between DFN and CPM models (Figure 3-2). In a combined DFN/CPM model the coupling is carried out with boundary conditions that give continuity of pressure or conservation of mass at the interface between the DFN and CPM domains. In our approach, the coupling is carried out by implementing a Cauchy-type boundary condition that ensures mass conservation at the interface.

The Cauchy boundary condition specifies that the mass flow per unit length of the intersection (q^{int}) is proportional to the pressure difference between the pressure in the fracture (p_f) and the pressure in the porous domain (p_m), and is given by

$$\begin{cases} q_f^{int} = -\alpha(p_m - p_f) & \text{in } L_{int} \\ q_m^{int} = \alpha(p_m - p_f) & \text{in } L_{int} \end{cases} \quad (3-15)$$

where L_{int} (m) is the length of the fracture in contact with the porous media. q_f^{int} (m/s) is the flow from the fracture to the porous medium and q_m^{int} (m/s) is the flow from the porous medium to the fracture. The coefficient of proportionality α (s) is referred to as a conductance or leakage coefficient in groundwater flow codes. Figure 3-3 shows the behaviour of the boundary condition as a function of α . The Cauchy boundary condition can cover the range between a prescribed pressure boundary condition ($\alpha = \infty$) and a no-flow boundary condition ($\alpha = 0$).

For values of α larger than a threshold α_p , the boundary condition behaves as a prescribed pressure (Dirichlet) boundary condition and the flow through the interface is independent of the value of α . For values of α lower than α_p , the boundary condition behaves as a prescribed flow (Neumann) boundary condition. The value of the flow in those cases depends on the value of α . As a result, there is a pressure discontinuity at the fracture-porous medium interface.

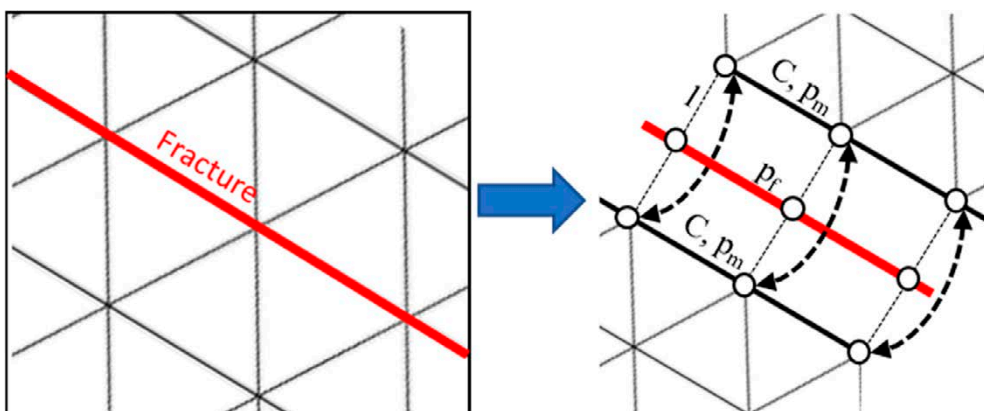


Figure 3-2. Scheme of a finite element mesh showing the numerical representation of the fracture/matrix exchange term for the groundwater flow and conservative transport coupling.

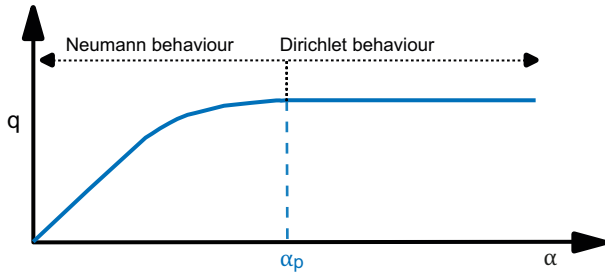


Figure 3-3. Behaviour of the Cauchy boundary condition as a function of the conductance α . The flow increases with the value of α until a threshold value (α_p) is reached. For values larger than α_p , the flow remains constant and the pressure in the fracture and in the matrix equal in shared nodes.

Assuming that there is a physical interface or “layer” between the porous medium and the fracture that is not explicitly modelled, the physical meaning of the coefficient of proportionality α can be extracted from Darcy’s law integrated over the fracture aperture d_f (m):

$$u_f = -d_f \frac{\rho k_{int}}{\mu} |\vec{\nabla} p| = -d_f \frac{\rho k_{int}}{\mu} \frac{\Delta p}{b_{int}} = -\overbrace{d_f \frac{\rho k_{int}}{\mu b_{int}}}^{\alpha} (p_f - p_m) \quad (3-16)$$

Where ρ (kg/m³) is the fluid density, k_{int} (m²) is the permeability at the interface between matrix and fracture and b_{int} (m) is the thickness of the “layer” between the porous medium and the fracture. The flow at the boundary depends on the properties of the interface. Thus, α is proportional to the permeability at the interface between the porous medium and the fracture, k_{int} , and inversely proportional to the thickness of the layer, b_{int} .

In the applications presented in this report, the α value is selected such that the boundary condition behaves as a Dirichlet boundary condition. In this case, the boundary condition provides both conservation of mass and continuity of pressure at the interface between the DFN and CPM domains. The boundary condition is applied where discrete fractures intersect the porous domains.

Conservative transport coupling

In a similar way, the coupling between the transport of species in solution in the fractures and the transport of diluted species in the porous medium ensures mass conservation. The solute mass flow per unit length of intersection entering the fracture, j_f^{int} (mol/m/s), equals the solute mass flow per unit length of intersection leaving the porous medium, j_m^{int} , or vice versa.

$$j_f^{int} + j_m^{int} = 0, \quad (3-17)$$

The coupling is carried out using a Cauchy-type boundary condition that specifies that the solute mass flow per unit length of intersection ($j_{f,m}^{int}$) is proportional to the difference in concentration in the fracture (c_f) and in the porous domain (c_m), that is:

$$\begin{cases} j_f^{int} = -\beta(c_m - c_f)\rho_l \text{ in } L_{int}, \\ j_m^{int} = \beta(c_m - c_f)\rho_l \text{ in } L_{int}, \end{cases} \quad (3-18)$$

where L_{int} (m) is the length of the fracture in contact with the porous media. The proportionality coefficient β (m²/s) is the mass transfer coefficient. There are different expressions for β in the literature. Here, the physical meaning of β can be extracted from Fick’s law integrated over the fracture aperture d_f (m) and applied to the length of the intersection between the porous medium and the discrete fractures L_{int} :

$$j^{int} = -d_f D_{int} |\vec{\nabla}_n c| \rho_l = -d_f D_{int} \frac{\Delta c}{b_{int}} \rho_l = -\overbrace{d_f D_{int}}^{\beta} (c_f - c_m) \rho_l \quad (3-19)$$

The value of β is proportional to both the diffusivity at the interface between the porous medium and the fracture, D_{int} , and the fracture aperture d_f and inversely proportional to the thickness of the layer, b_{int} .

As in the groundwater flow coupling, if β is large enough, the coupled set of equations will yield similar concentration values in the fracture and the porous medium domains. In that case, the Cauchy or mixed boundary condition behaves as a Dirichlet-type boundary condition. Then, the mass exchange between the matrix and fracture would be well defined and would not depend on the value of β . However, if β is lower than a given threshold, the exchange term behaves as a Neumann-type boundary condition. In this case, the mass exchange between the two domains would strongly depend on β and the tracer concentrations in the porous domain and at the fracture nodes would diverge, i.e., there would be no concentration continuity at the fracture-matrix interface. Therefore, the mass exchange is bounded between zero, when β is zero and the maximum mass exchange value, reached when β tends to infinity.

For the applications presented in this work, the value of β is selected so that the boundary condition behaves as a Dirichlet boundary condition. Thus, the boundary condition provides both conservation of mass and continuity of concentration at the interface between the DFN and CPM domains.

3.2.4 Chemical reaction modelling

The chemical part of the reactive transport problem is performed using PHREEQC which solves a set of algebraic differential equations. The reactive system consists of a set of ordinary differential equations representing kinetic reactions:

$$\begin{cases} \frac{du_g}{dt} + \frac{du_m}{dt} + \frac{du_a}{dt} + \frac{du_d}{dt} = r_{kin} \\ f(u, c, r_{kin}, T) = 0 \end{cases} \quad (3-20)$$

where $u = U_c$ (mol/kg_w) is the vector of components, U is the component matrix and T (°C) is the temperature. The subscripts refer to the subcomponent in phase gas (g), mineral (m), aqueous (a) and sorbed (d), respectively. Thus, the conservative concentrations of the dissolved species computed in Equations (3-11) and (3-13) are included as u_a in Equation (3-20).

The chemical system solved in PHREEQC consists of a set of ordinary differential equations (ODE) associated with kinetic reactions, and a set of algebraic equations which arise from the formulation of components u , the mass action law, the water activity model used to represent non-ideal solutions, etc. Furthermore, PHREEQC also includes the usually non-linear expressions that relate u , c , and r_{kin} and also T (for non-isothermal problems). The complete formulation can be found in the PHREEQC User's Guide (Parkhurst and Appelo 2013).

4 Results

A reactive transport model involves coupling of groundwater flow, transport of diluted species and biogeochemical reactions. The flow and solute transport in fractured porous media are modelled using COMSOL Multiphysics (COMSOL 2017). To verify the implementation in COMSOL, a number of benchmark problems are solved, and the results of the calculations are discussed in Sections 4.1 and 4.2. In Section 4.3, the new version of iCP is used to solve a set of reactive problems of increasing complexity. First, a problem of reactive transport in a discrete fracture is solved. Second, the reactive transport in a hydrological system with discrete fractures embedded in a reactive porous medium (hybrid method) is considered.

4.1 Groundwater flow

The benchmarking cases proposed to validate the groundwater flow equation implementation in COMSOL are reported in Flemisch et al. (2018). Here, the authors propose four different benchmarking problems. They offer a comparison of results obtained with different software using different numerical methods or approaches to solve groundwater flow in fractured media. The four benchmarking cases have been reproduced using COMSOL and the results are presented and discussed in this section.

Table 4-1 summarizes the methods used by different software programs to conceptualize the fractures. It describes whether the fracture is represented as an element of 1 dimension lower than the porous domain (edges in a 2D surface) or as an element of the same dimension (surfaces in 2D domains). It indicates where the dependent variable is evaluated (vertex or element) and whether the numerical method assumes continuity of the dependent variable at the model interfaces or not. This characteristic becomes relevant to represent fractures less permeable than the porous matrix, as described in detail in Section 4.1.3.

Table 4-1. Numerical methods to solve flow in fractured porous media reported in Flemisch et al. (2018).

Method	Degrees of freedom	Fracture dimension	Conforming	Pressure continuity
Box-DFM	p (vertex)	dim-1	Yes	Yes
CC-DFM	p (element)	dim-1	Yes	No
EDFM	p (element)	dim-1	No	Yes
mortar-DFM	p (element), u (faces)	dim-1	Geometrically	No
P-XFEM	p (vertex)	dim-1	No	No
D-XFEM	p (element), u (faces)	dim-1	No	No
MFD	p (faces)	Dim	Geometrically	No

4.1.1 Benchmark 1 – Hydrocoin

Problem description

This problem is based on the international Hydrocoin project (OECD 1987). Figure 4-1 shows the model geometry and parameters. This problem considers a 2D cross-section with an irregular shape. The system includes two high conductive fractures crossing a crystalline rock. A hydraulic head equal to the elevation is prescribed on the top surface (Dirichlet boundary condition) and the rest of boundaries are no-flow boundaries. The comparison between software is carried out by comparing the hydraulic head obtained along a horizontal line located at $z = -200$ m (dashed blue line in Figure 4-1). The positions of vertexes are listed in Table 4-2.

Table 4-2. Coordinates of domain vertices.

vertex no	x(m)	z(m)	vertex no	x(m)	z(m)
1	0	150	11	1505	-1000
2	394.28	100.71	12	1495	-1000
3	400	100	13	1007.5	-1000
4	404.44	100.55	14	992.5	-1000
5	800	150	15	0	-1000
6	1192.66	100.91	16	1071.34	-566.34
7	1200	100	17	1084.03	-579.03
8	1207.67	100.95	18	1082.5	-587.5
9	1600	150	19	1069.80	-574.80
10	1600	-1000			

This benchmark includes the simplest geometry and mesh of the four cases considered in Flemisch et al. (2018). The groundwater flow computed using COMSOL Multiphysics is compared against the results of all the other methods listed in Table 4-1.

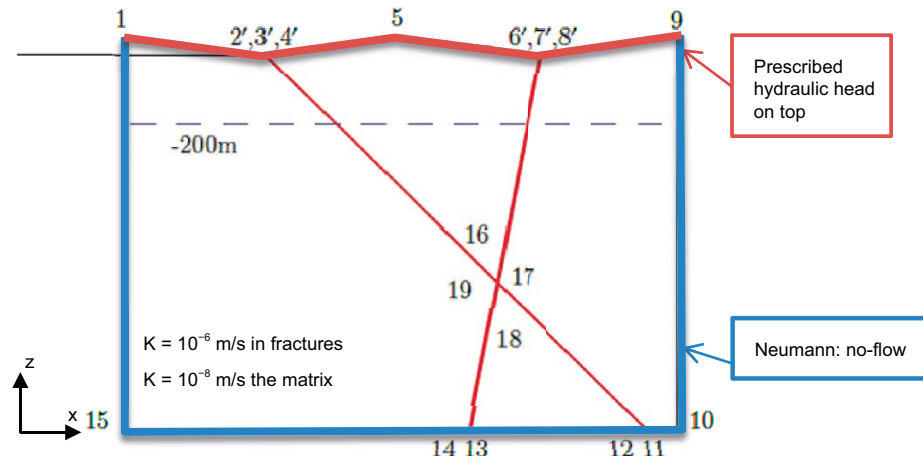


Figure 4-1. Geometry and model parameters of benchmark problem number 1. The blue dashed line shows the depth at which the computational results of the codes are compared. Figure modified from OECD (1987).

Results

The solution shows a hydraulic gradient from the high topographic areas to the lower areas (Figure 4-2). Most part of the flow occurs near the upper boundary. The highly permeable fractures dominate the groundwater flow and constrain the regional flow field. The fractures intersect the upper boundary in the low topographic positions. Therefore, fractures represent preferential paths for the groundwater discharge.

Figure 4-3 shows the hydraulic head along a line at a depth of 200 m computed at steady state by COMSOL Multiphysics and the other methods. The smooth solution obtained using COMSOL is in good agreement with the reference results and those from other methods. Only the results of the EDFM method deviates from the results of the other codes due to the type of elements and the lower mesh resolution.

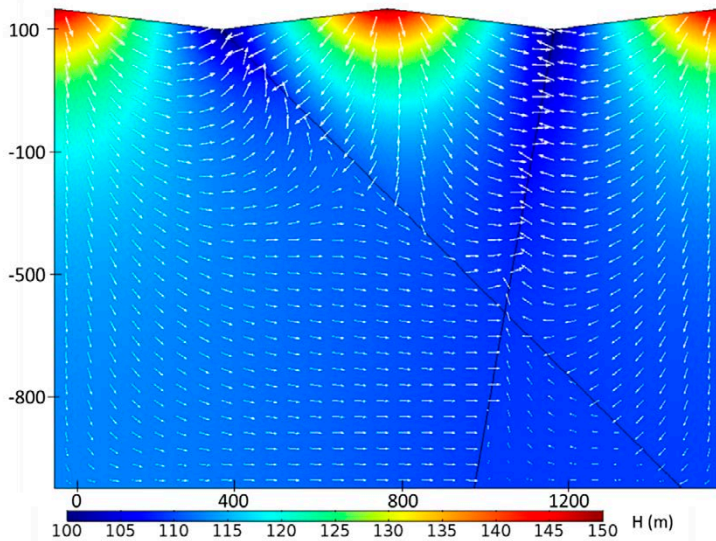


Figure 4-2. Computed hydraulic head and vectors showing the flow direction.

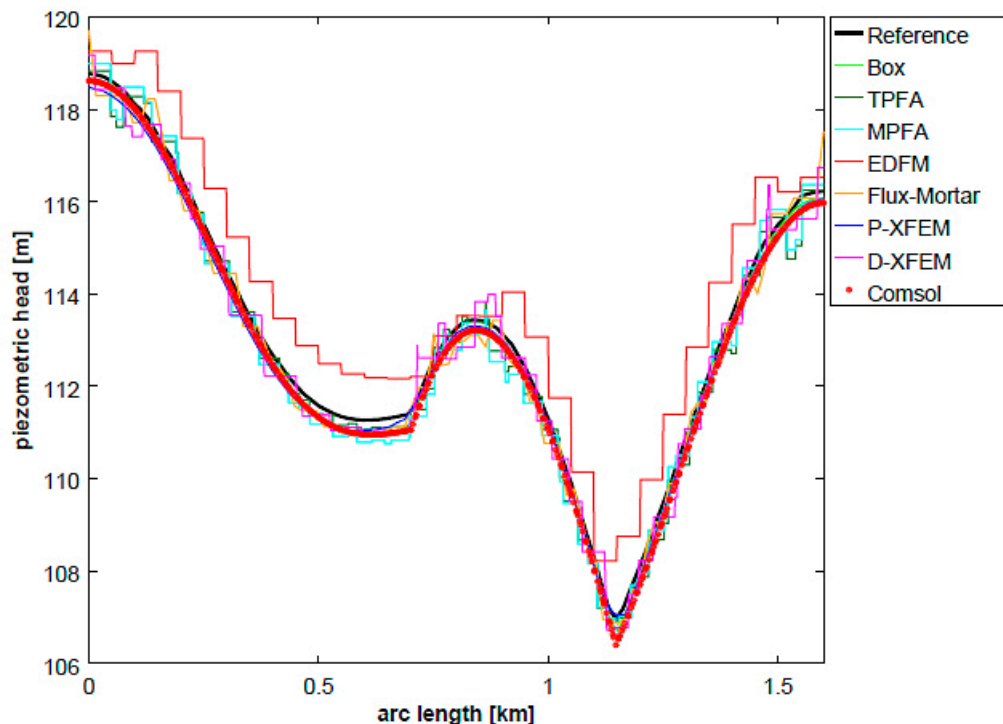


Figure 4-3. Comparison of the computed hydraulic head along a horizontal line at a depth of 200 m.

4.1.2 Benchmark 2 – Regular fracture network

Problem description

The second benchmark is based on Geiger et al. (2013) with a slightly modified boundary condition. The domain includes a fracture network (red lines in Figure 4-4) and a matrix domain. The isotropic permeability of the matrix is 1 m^2 . The aperture of the fractures is assumed to be uniform and equal to $1 \times 10^{-4} \text{ m}$. Two different cases are considered in this benchmark. The first case considers highly permeable fractures with permeability equal to $1 \times 10^4 \text{ m}^2$ and the second case low permeable fractures with permeability equal to $1 \times 10^{-4} \text{ m}^2$. The benchmarking of the case with high permeable fractures is carried out by comparing the pressure distribution along two lines: a vertical line at $x = 0.5 \text{ m}$ and a horizontal line at $y = 0.7 \text{ m}$. The benchmarking of the case with low permeable fractures is carried out by comparing the pressure distribution along a diagonal line from the point $x = 0.0 \text{ m}, y = 0.1 \text{ m}$ to $x = 0.9 \text{ m}, y = 1.0 \text{ m}$.

The main difficulty associated with this benchmark is the ability to deal with low permeable fractures. In this case, the fractures should act as flow barriers generating pressure jumps in the matrix pressure distribution. Several of the most common numerical methods cannot describe these jumps. Instead, continuity of the pressure field across the fracture has been assumed and incorporated into the method. The consequences of this assumption on the computational results will be discussed in more detail in the following section.

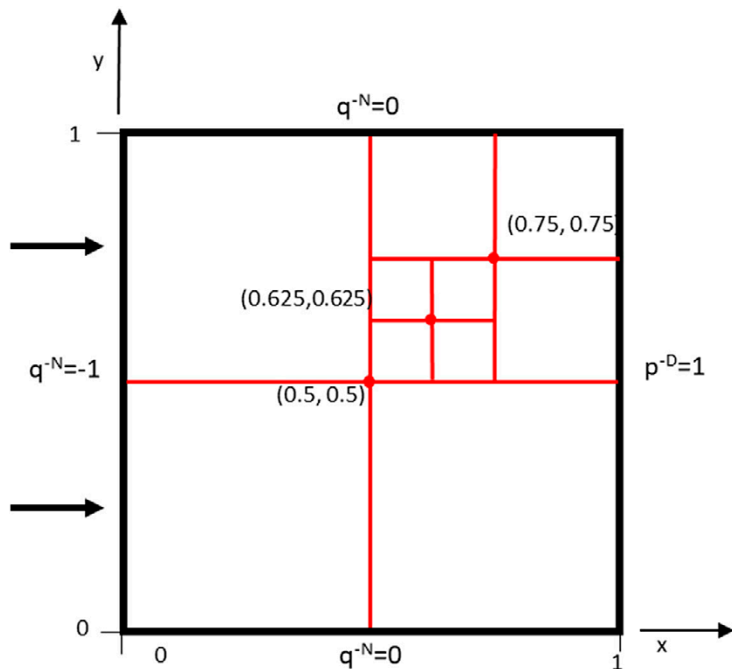


Figure 4-4. Geometry and boundary conditions (modified from Flemisch et al. 2018).

Results

Figure 4-5 shows the pressure field obtained for the case with high permeable fractures. The highest pressures are found at the top and bottom of the left boundary. Most flow is directed towards the horizontal fractures (Figure 4-5). Figure 4-6 shows a comparison between the COMSOL results and the results reported in Flemisch et al. (2018). The COMSOL solution fits the results obtained with most of the other methods. The solution exhibits continuity in the pressure distribution.

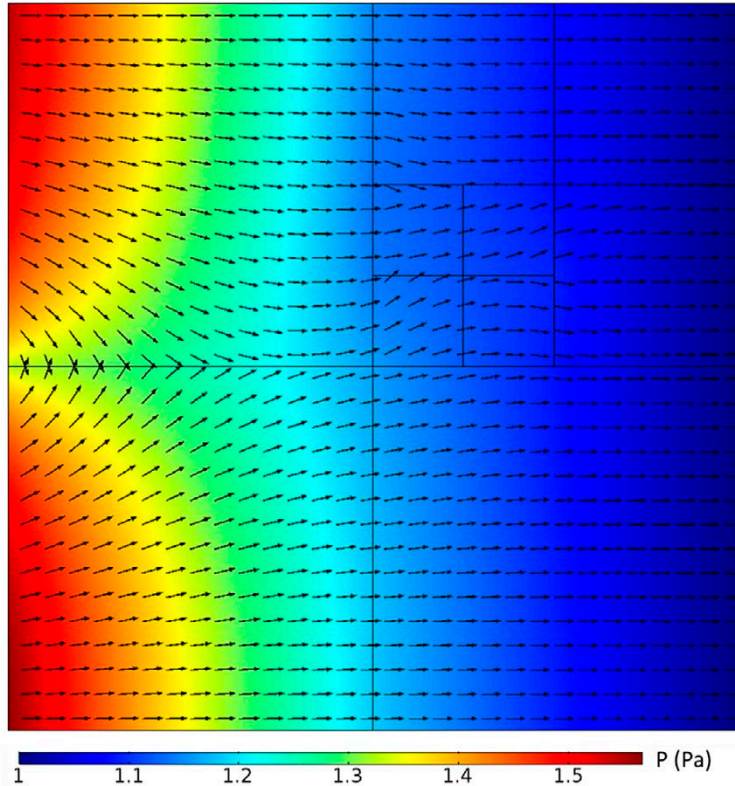


Figure 4-5. The pressure field with vectors showing the flow direction for the case with fracture more permeable than the matrix.

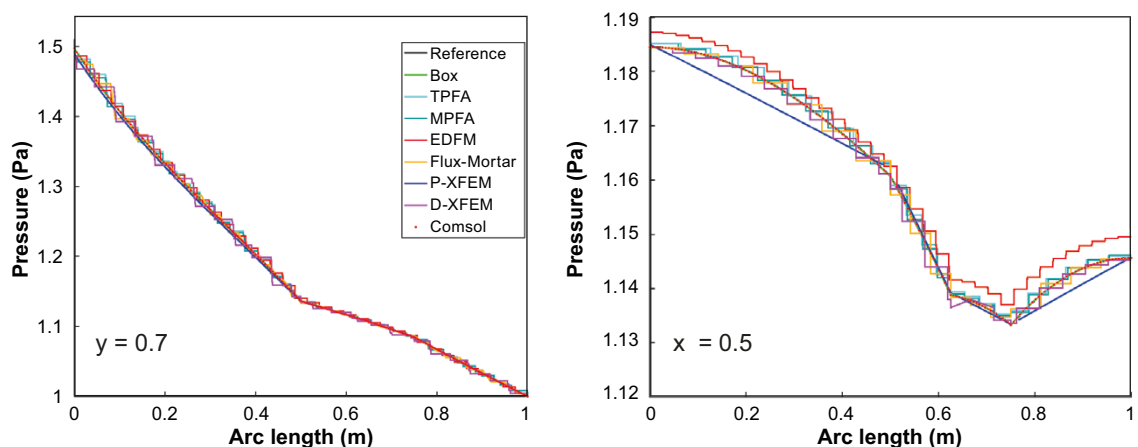


Figure 4-6. Pressure values along a horizontal line at $y = 0.7$ m and a vertical line at $x = 0.5$ m for the case with high permeability fractures.

Figure 4-7 shows a comparison of the results for the case with low permeability fractures. In this case, COMSOL does not reproduce a correct solution to the problem. It shows similar results to those obtained with the EDFM code. This is because both COMSOL and the EDFM code assume pressure continuity. This imposes that the computed pressure must be the same for the fracture and the two porous medium nodes located next to the fracture. Therefore, although the fractures have low permeability, they do not act as a flow barrier because the pressure is the same in the matrix at both sides of the fracture. The formulation does not allow for sharp pressure changes as the ones observed in Figure 4-7. However, this problem is not so relevant in the case of fractured crystalline rocks because the most important fractures in a safety assessment are more permeable than the surrounding matrix.

The default settings to solve groundwater flow in fractured media in COMSOL Multiphysics do not allow to simulate properly low permeable fractures. However, the effect of the low permeability fractures can be effectively modelled using a “thin barrier” boundary condition at the fractures. This boundary condition imposes flows through the fracture-matrix interface applying an approximate analytical solution. In this case the flow through the low permeable fracture is computed using Darcy’s law on the form:

$$q_t = \frac{k_f \rho g}{\mu} \frac{p_{\text{up}} - p_{\text{down}}}{d} \quad (4-1)$$

where q_t (m/s) is the flow perpendicular to the fracture, k_f (m^2) is the fracture permeability, ρ (kg/m^3) is the fluid density, μ ($\text{Pa}\cdot\text{s}$) is the viscosity, p_{up} and p_{down} is the fluid pressure upstream and downstream respectively and d (m) is the thickness of the fracture. The pressure is the dependent variable governed by the partial differential equation.

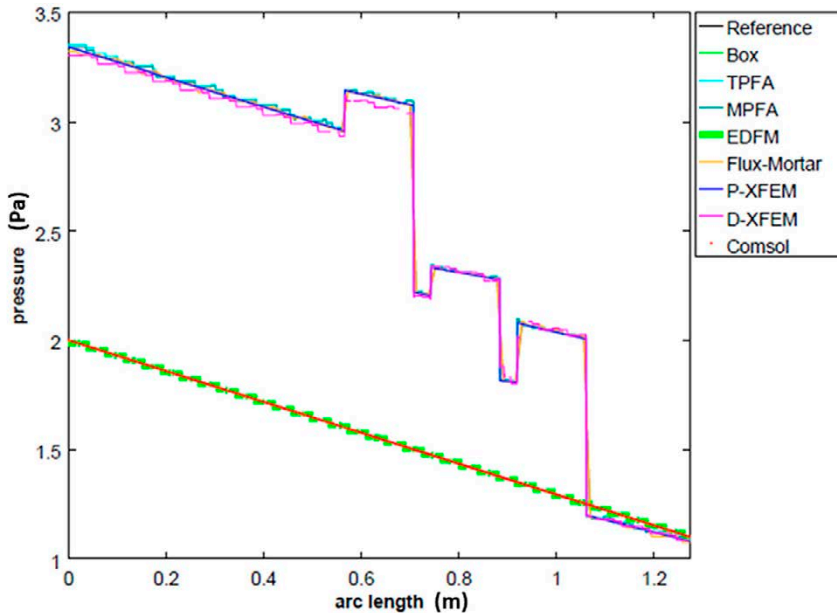


Figure 4-7. Pressure values along a diagonal line from (0.0, 0.1) to (0.9, 1.0) for the case with low permeable fractures.

Using this approach, the resulting solution matches the correct ones obtained with other methods (Figure 4-8). The resulting pressure field shows the expected sharp pressure jumps at both sides of the semi-impermeable fractures (Figure 4-9).

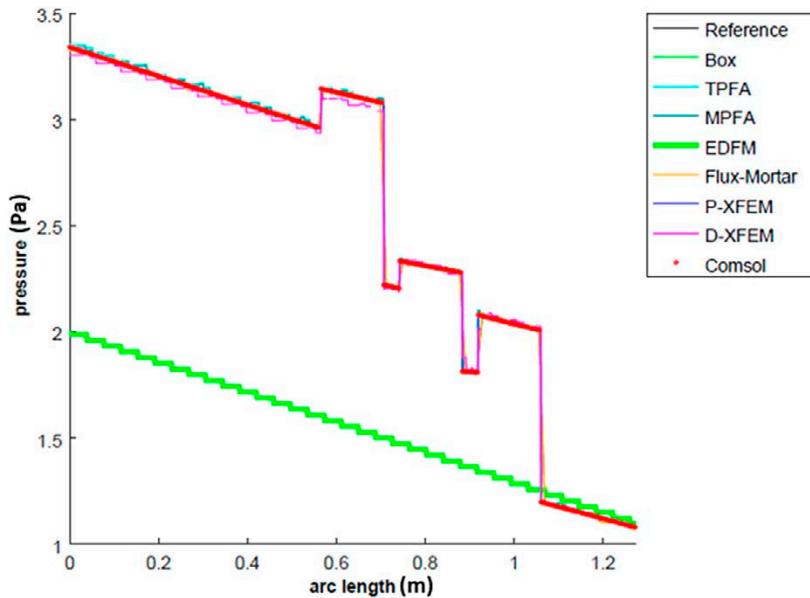


Figure 4-8. Pressure values along a diagonal line from (0.0, 0.1) to (0.9, 1.0) for the case with low permeability fractures.

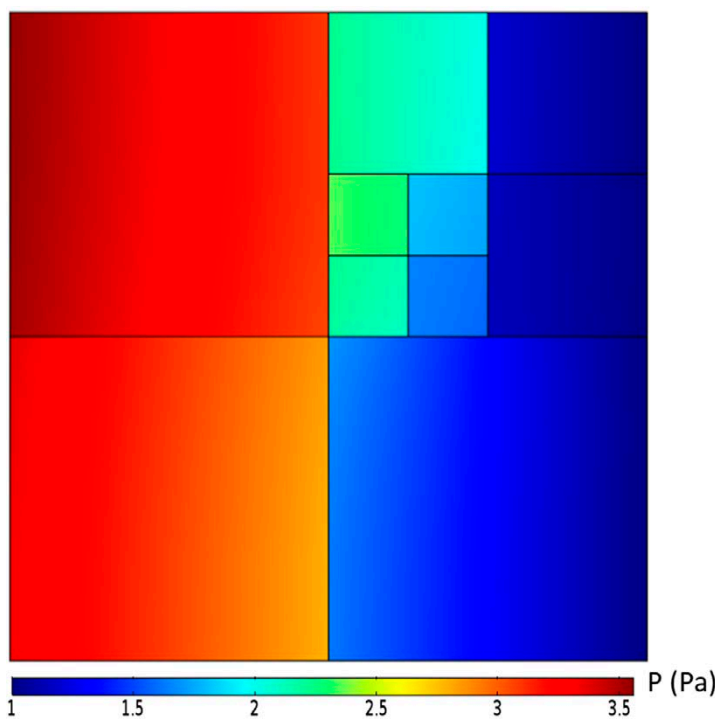


Figure 4-9. Pressure distribution in the porous material for the case with fracture less permeable than the matrix.

4.1.3 Benchmark 3 – Complex fracture network

Problem description

The third benchmark model represents a set of fractures with different permeability in a matrix domain of $1 \times 1 \text{ m}^2$ (Figure 4-10). As in the previous case, the permeability of the matrix is set to 1 m^2 . For the fractures, the permeability ranges from $1 \times 10^4 \text{ m}^2$ to $1 \times 10^{-4} \text{ m}^2$. The aperture is assumed to be constant for all the fractures and equal to $1 \times 10^{-4} \text{ m}$. Two flow configurations are considered: the first with a vertical gradient from top to bottom (left in Figure 4-10) and the second with horizontal pressure gradient from left to right (right panel in Figure 4-10). Table 4-3 shows the coordinates of the fracture endpoints whereas the permeability of the fractures is shown in Figure 4-10. The results on a line between point $(0.0, 0.5)$ and $(1.0, 0.9)$ in Figure 4-10 were compared.

Table 4-3. Coordinates of the different fracture endpoints (Flemisch et al. 2018).

Fracture no	x_{left}	y_{left}	x_{right}	y_{right}
1	0.05	0.416	0.22	0.0624
2	0.05	0.275	0.25	0.135
3	0.15	0.63	0.45	0.09
4	0.15	0.9167	0.4	0.5
5	0.65	0.8333	0.85	0.1667
6	0.7	0.235	0.85	0.1675
7	0.6	0.38	0.85	0.2675
8	0.35	0.9714	0.8	0.7143
9	0.75	0.9574	0.95	0.8155
10	0.15	0.8363	0.4	0.9727

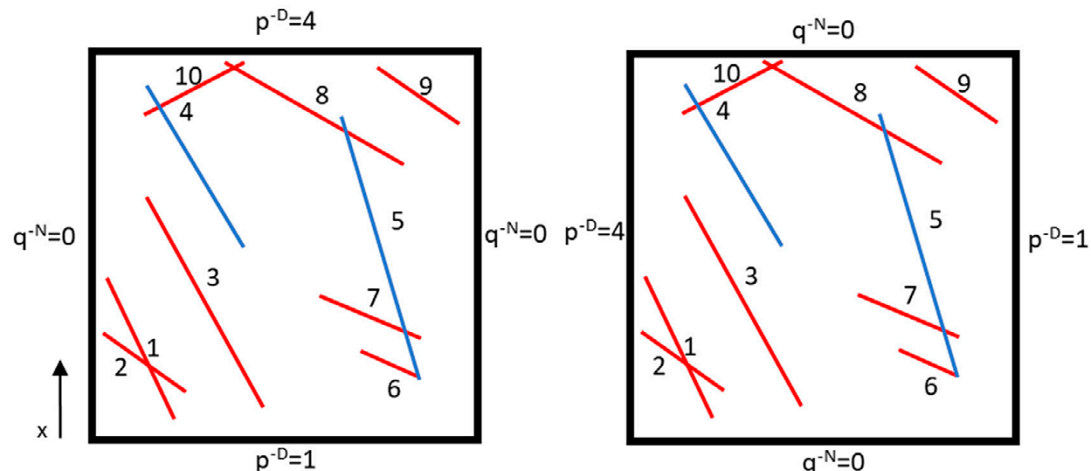


Figure 4-10. Geometry and boundary conditions. Red fractures are conductive, and blue have low permeability (modified from Flemisch et al. 2018).

Results

In both flow configurations, the obtained pressure field is mainly controlled by the high permeable fractures (Figure 4-11). The sub-vertical fractures act as preferential flow paths for the groundwater in both cases. The effect of the fractures on the groundwater flow strongly depends on the fracture orientation. The fractures oriented parallel to the pressure gradient act as preferential flow paths and modify the groundwater flow field, as shown by the velocity vectors in Figure 4-11.

The reference results differ from those obtained with COMSOL. The reference results show abrupt pressure changes near low permeable fractures (blue fractures in Figure 4-10), whereas COMSOL results show smoother pressure changes. The differences between COMSOL and the reference results are restricted to the low permeability fractures. The global pressure field is similar for all methods, as shown in Figure 4-12. The main differences are located at points where the observation lines traverse the low permeability fractures.

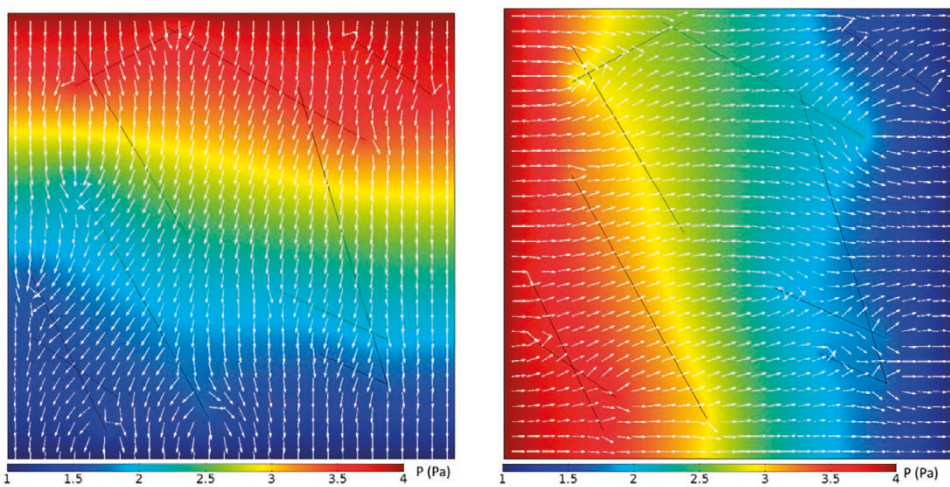


Figure 4-11. Pressure field and vectors showing the flow direction for the vertical flow case (left) and the horizontal flow case (right).

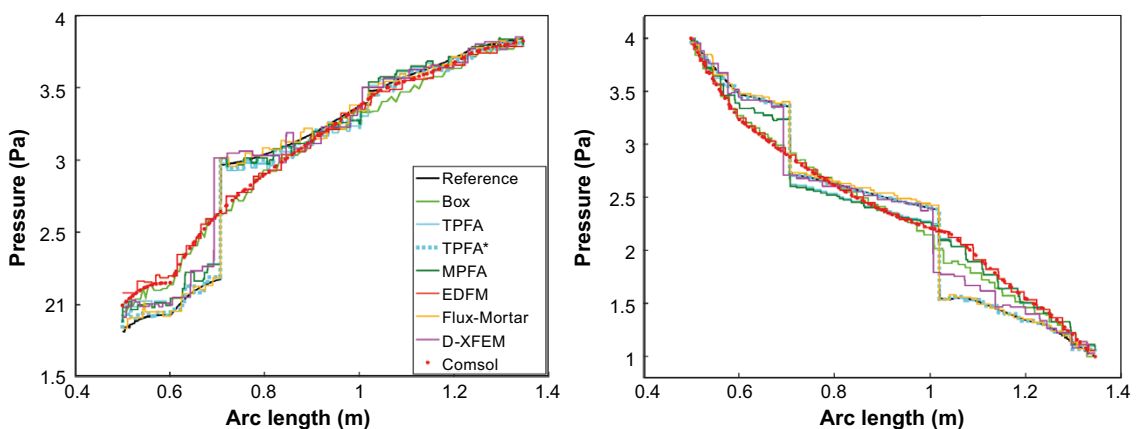


Figure 4-12. Comparison of the pressure distribution calculated with the different methods and the results obtained using COMSOL Multiphysics. Case with vertical pressure gradient (left) and case with horizontal pressure gradient (right).

As in previous benchmarks, these results indicate that COMSOL, using the default settings to solve flow in fractured media, does not reproduce the effect of low permeability fractures. However, if the global effect of the low permeability fractures on the flow field is not very important, COMSOL results approximate accurately the solution.

As in the previous benchmark, the low permeable fractures can be accurately described using the thin barrier boundary condition Equation (4-1). Using this boundary condition, the resulting pressure field (shown in Figure 4-13) fits the reference results. The pressure distribution along a line is shown in Figure 4-14. A very good agreement is observed between the modified COMSOL results and the results from the other methods that can handle low permeable fractures.

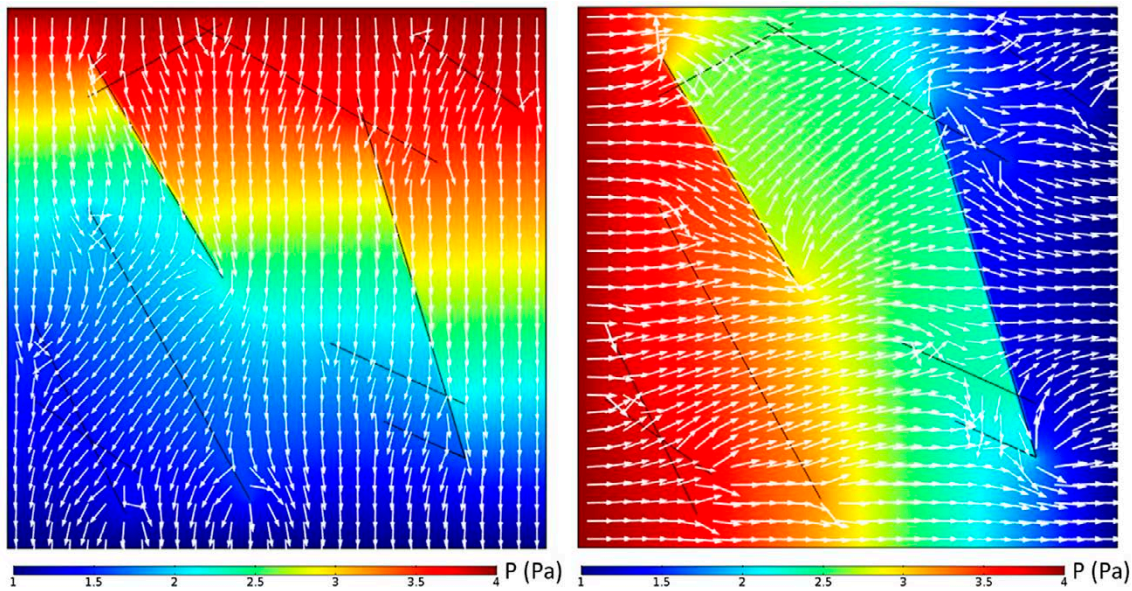


Figure 4-13. Pressure field and vectors showing the flow direction for the horizontal flow case (left) and the vertical flow case (right) for the simulation that uses the “thin barrier” boundary condition.

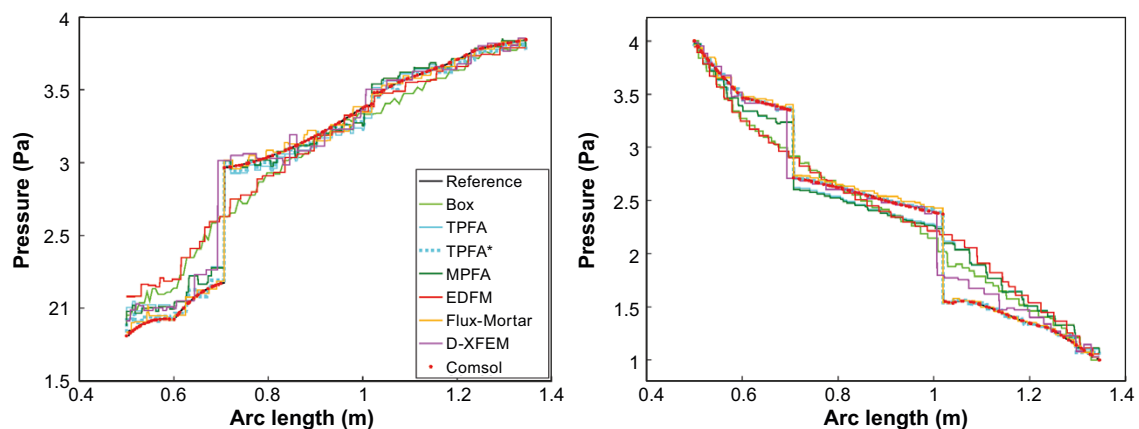


Figure 4-14. Pressure distribution computed with COMSOL using the “Thin barrier” boundary condition at the fractures and the results from the other methods. Case with vertical gradient (left) and case with horizontal gradient (right).

4.1.4 Benchmark 4 – Case based on outcrop data

Problem description

The last flow benchmark considers a case based on a real set of fractures taken from an outcrop located in Norway. The geometry of the fractures and the model are depicted in Figure 4-15. The domain is a rectangle of $700 \times 600 \text{ m}^2$ formed by a porous matrix and a set of discrete fractures. The porous matrix has a uniform scalar permeability equal to $1 \times 10^{-14} \text{ m}^2$. The permeability of the fractures is constant and equal to $1 \times 10^{-8} \text{ m}^2$ with an aperture of 10^{-2} m . Regarding the boundary conditions, a no flow boundary condition is imposed at the top and bottom boundaries and a Dirichlet boundary condition is imposed at the left and right boundaries with a pressure of 1 013 250 Pa and 0 Pa, respectively. The spatial configuration of the fractures has been slightly modified to generate linear fractures.

The comparison of the solution obtained with the different methods is carried out by presenting the spatial distribution of the pressure along two different lines: a horizontal line at $y = 500 \text{ m}$ and a vertical line at $x = 625 \text{ m}$.

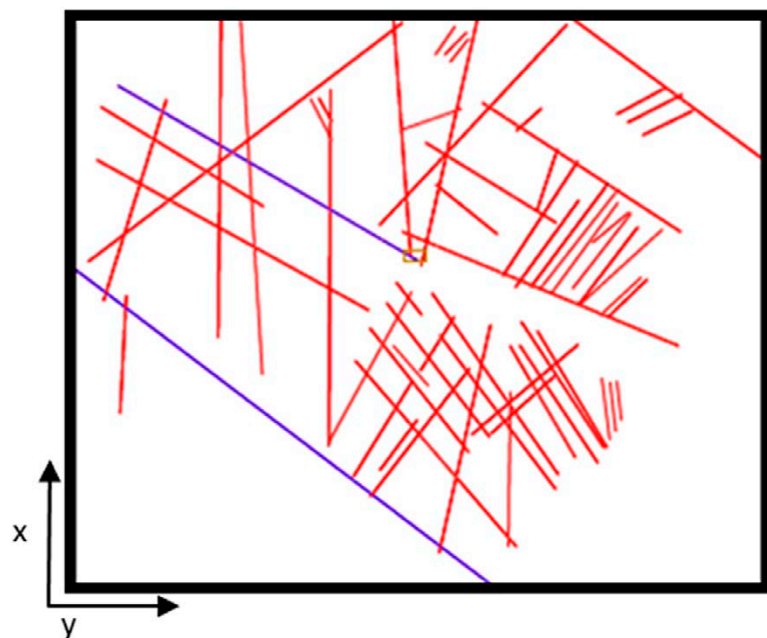


Figure 4-15. Geometry of the model with discrete fractures (blue and red lines) embedded in a porous medium (white). The blue lines show fractures that have been rectified (modified from Flemisch et al. 2018).

Results

The resulting pressure field for this problem is presented in Figure 4-16. The modelled area can be divided in two parts: the larger part of the domain that is covered by a high density of fractures (high hydraulic head areas in Figure 4-16) and the area with a lower density of fractures. The pressure gradient is small in the areas with high fracture density. Most part of the domain has a hydraulic head between 100 and 80 m (Figure 4-16). This area coincides with the area with a high presence of fractures. However, next to the right boundary there are few fractures, and the hydraulic gradient is larger than the one in the highly fractured area.

The comparison with the other methods is shown in Figure 4-17. Note that COMSOL results are consistent with those from other methods. Therefore, it can be concluded that COMSOL can handle complex fracture geometries and provide accurate results.

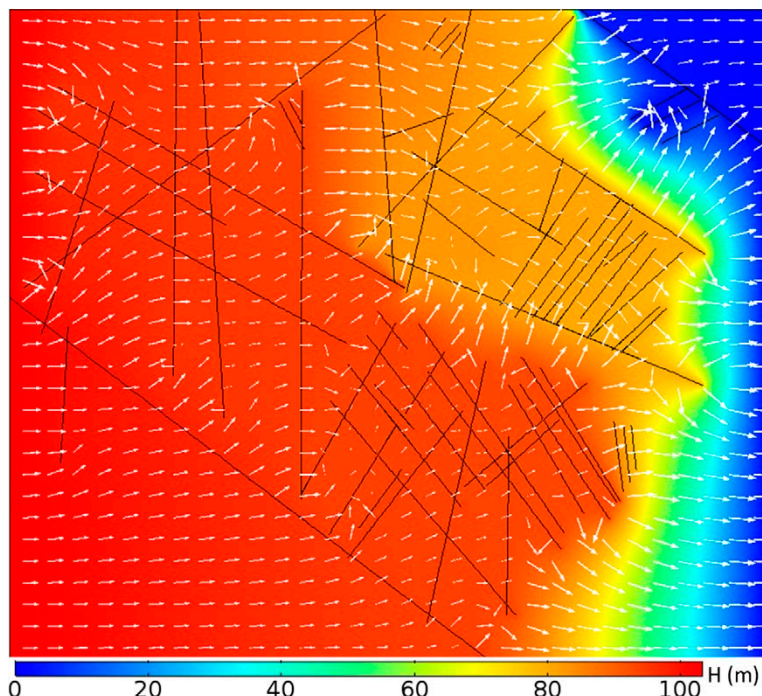


Figure 4-16. Representation of the pressure field obtained for the case based on outcrop data in COMSOL. White arrows show the flow direction in the matrix. The arrow length is proportional to the Darcy flow velocity.

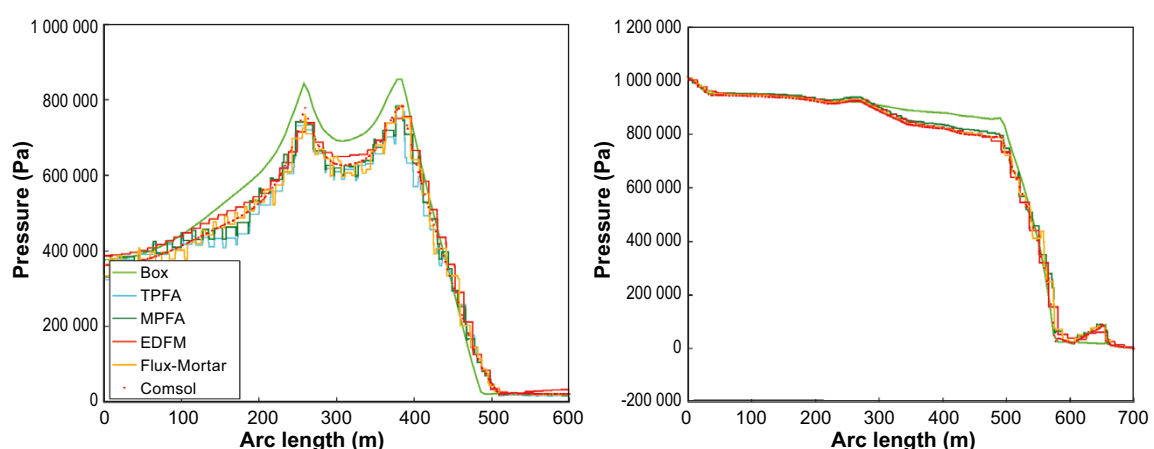


Figure 4-17. Pressure solutions of the different methods for lines $y = 500$ (left) and $x = 625$ m (right).

4.2 Conservative transport

4.2.1 Contaminant transport through a fracture with matrix diffusion

Problem description

The analytical solution proposed by Tang et al. (1981) for the transport of a tracer through a fracture affected by matrix diffusion is used to test the implementation of the non-reactive transport in fractures in COMSOL Multiphysics. This analytical solution has been used to test codes such as Pflotran (Hammond and Lichtner 2010) and PHAST (Parkhurst et al. 2004).

The modelled system consists of a 100-m long fracture and a matrix domain of size $1 \times 100 \text{ m}^2$ (Figure 4-18). The domain is symmetrical along the fracture. Thus, one-half the fracture aperture width, which is 0.1 m, is explicitly included in the model. Transport in the fracture is dominated by advection from left to right with a flow velocity of 5 m/year. Transport in the matrix is governed by diffusion with an effective diffusivity of $1 \times 10^{-14} \text{ m}^2/\text{s}$. The fracture and matrix porosity values are 0.5 and 0.001 ($\text{m}^3_{\text{water}}/\text{m}^3_{\text{medium}}$), respectively.

The water enters through the left fracture boundary. A fixed tracer concentration equal to 1 is applied at the left boundary of the fracture. An outflow boundary condition is applied over the right boundary of the fracture. A no-flow boundary condition is imposed at the rest of the boundaries. The transient tracer transport is simulated for 10 000 years.

This model is conceptualized in COMSOL using different matrix and fracture dimensions (Figure 4-19):

- A. 3D continuous porous media (3D CPM). Both the matrix and the fracture are considered as 3D domains with one element in the y-direction. Thus, the fracture is modelled as a continuous 3D porous medium.
- B. Hybrid 3D-2D domains (Hybrid 3D2D). The matrix is considered as a 3D domain with one element in the y-direction, and the fracture is defined as a 2D discrete fracture. Therefore, this configuration employs a hybrid method with 3D porous materials and 2D discrete features.
- C. 2D continuous porous media (2D CPM). The matrix and the fracture are represented by two different 2D domains. This configuration uses a continuous porous medium approach.
- D. Hybrid 2D-1D domains (Hybrid 2D1D). The matrix is considered as a 2D domain with a 1D discrete fracture. In this case, the model uses a hybrid method with a 2D matrix and 1D discrete fracture.
- E. Extra dimension. The fracture is represented by one 1D discrete element and the matrix is represented by an extra-dimension.

The validation of the model implementation in COMSOL is carried out by comparing the breakthrough curve at the fracture outlet with those computed by Pflotran, PHAST and the analytical solution presented by Tang et al. (1981).

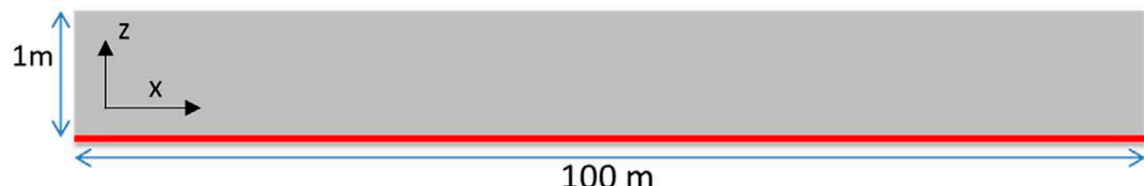


Figure 4-18. Geometry of modelled system. The red line illustrates the fracture and the grey field, the matrix domain.

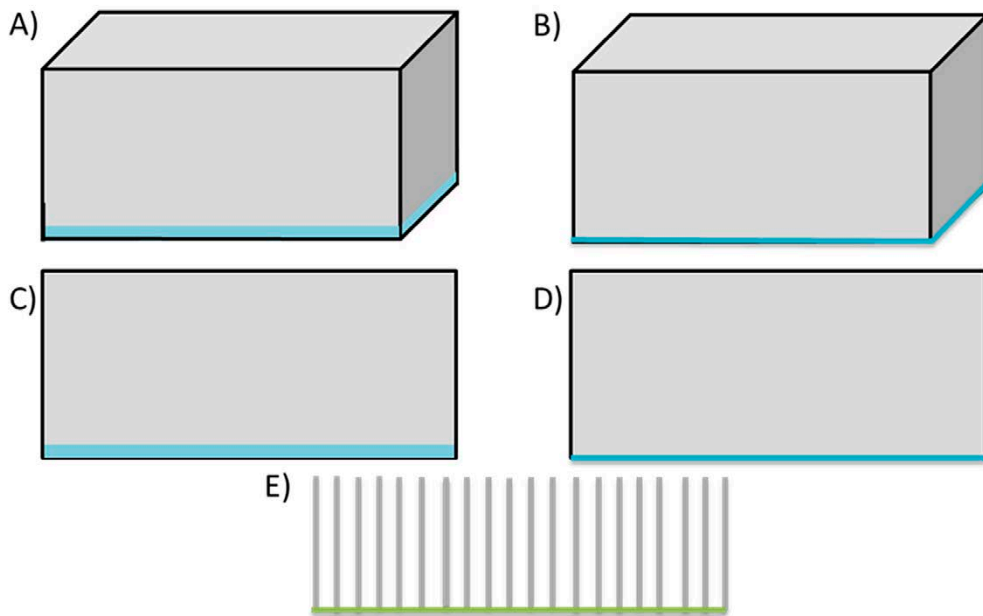


Figure 4-19. Different conceptualizations of the matrix and fracture, A) 3D matrix with a 3D fracture, B) 3D matrix with a 2D discrete fracture, C) 2D matrix with a 2D fracture, D) 2D matrix with a 1D discrete fracture, and E) 1D discrete fracture with extra-dimensions.

Results

The results for the transport of a conservative tracer are compared against the analytical solution by Tang et al. (1981) in terms of the normalized concentration vs. time (breakthrough curve) at the outlet of the fracture (Figure 4-20). Note that all numerical results are in a very good agreement for the first 750 years. However, after this time, numerical results show a significant increase in the tracer concentration with respect to the analytical solution. This is because after this specific time in all numerical simulations the tracer reaches the model boundary, and the analytical solution assumes that the rock matrix is infinitely large in the direction perpendicular to the fracture.

Table 4-4 shows the degrees of freedom and the computation time in COMSOL Multiphysics for the numerical representations A–D in Figure 4-19. The fastest simulation corresponds to the case of a 1D discrete fracture and a 2D matrix domain. Case E shows the results of the simulation where the matrix is conceptualized as an extra dimension. The results are equivalent to the ones obtained in cases A–D. This simulation was carried out on a different computer and, hence, the computation times are not comparable. The extra dimension method should be the most efficient method because it does not require meshing the whole matrix domain. This method will be useful for complex fracture network configurations where the matrix domain is difficult to mesh.

Table 4-4. Computer speed-up and degrees of freedom for the different model configurations implemented in COMSOL Multiphysics.

Model	Number of degrees of freedom	Execution time (s)
3D matrix 3D fracture	23517	423
3D matrix 2D fracture	22311	53
2D matrix 2D fracture	20703	38
2D matrix 1D fracture	20301	36

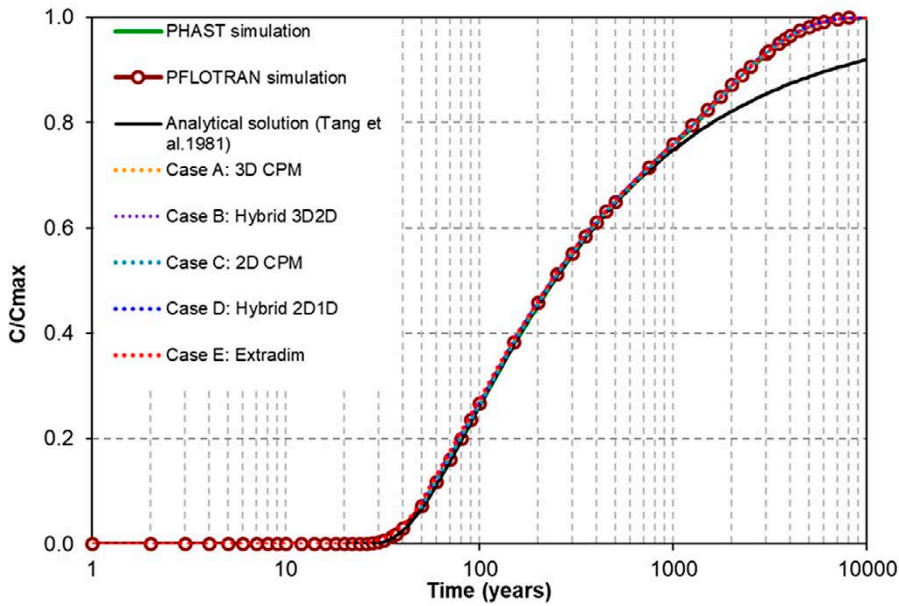


Figure 4-20. Breakthrough curves of normalized tracer concentration (C/C_{max}) at the fracture outlet ($x = 100$ m). Pflotran results (red circles), analytical solution (black line) and numerical results from COMSOL for the different geometrical conceptualizations are shown.

iCP

This problem has been solved also with the new version of iCP, which is able to perform reactive transport simulations in hybrid fractured media. In this case, this problem does not include reactions and only simulates the conservative transport of chloride. This simulation is used to verify that the implemented transport equation in the new version of iCP works correctly with the hybrid formulation (matrix + discrete fracture). The chloride concentration at the outlet point is compared with the one obtained with Pflotran (Figure 4-21). The iCP results are identical to those from other transport codes.

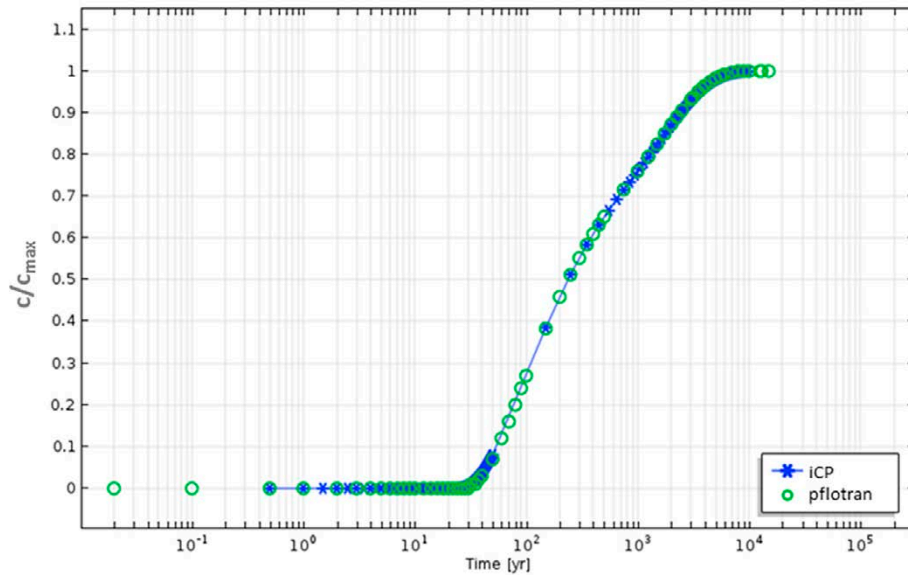


Figure 4-21. Breakthrough curves of normalized tracer concentration (C/C_{max}) at the fracture outlet ($x = 100$ m). Pflotran results (green circles) and iCP results (blue line).

4.3 Reactive transport

4.3.1 Pure DFN

Problem description

The proposed validation model is based on example 3 “Cation Exchange” in the iCP User’s Guide (Nardi et al. 2020). This example is based on example 11 in the PHREEQC User’s Guide (Parkhurst et al. 2013) and has been widely used as a benchmark problem (e.g. Kolditz et al. 2012). iCP results have been compared with result obtained using PHREEQC, PHAST and CRUNCHFLOW. In PHREEQC, PHAST and CRUNCHFLOW a 1D domain was modelled, whereas to validate the pure DFN approach implementation (Figure 2-2) a 2D fracture was modelled in iCP.

The transport of solutes in a saturated flow column is simulated. Cations are subject to cation exchange. The column initially contains a sodium-potassium-nitrate solution, and it is flushed with three pore volumes of a calcium chloride solution. A sketch of the problem and parameters values used are shown in Figure 4-22.

Results

Figure 4-23 shows a comparison between the results obtained with PHREEQC and the ones obtained with iCP solving the transport problem in a discrete fracture. The figure shows the comparison of the aqueous species calcium, chloride, sodium, potassium and nitrogen. A very good agreement between results is shown. In the simulation, chloride is a conservative solute and reaches the outlet of the fracture after approximately 52 000 seconds. The sodium cations initially present in solution or retained due to the cation-exchange capacity in the column are gradually replaced by incoming calcium cations and eluted. The midpoint of the breakthrough curve for sodium occurs at about 45 000 seconds. Because potassium cations bind more strongly than sodium cations (larger log K in the exchange reaction) to the column, potassium is released after sodium. Finally, when all the potassium has been released, the concentration of calcium increases to a steady-state value equal to the concentration in the infilling solution (at 70 000 seconds). In addition, the breakthrough curve of the chloride is compared to the analytical solution of the advection dispersion equation (ADE) (Bear 1972) proposed by Ogata and Banks (1961).

4.3.2 Hybrid method – Reactive fractures and matrix

iCP is finally applied to a reactive transport problem involving fractures embedded in a porous matrix where the precipitation/dissolution of minerals takes place in both the fractures and the matrix. The model conceptualizes the fracture as an independent chemical domain. The coupled reactive transport formulation is used to solve the flow and transport problem proposed by Martinez-Landa et al. (2012).

Martinez-Landa et al. (2012) present a hybrid model to study calcite precipitation in fractures, driven by the mixing of granitic waters and pore-water leached from concrete. However, this study does not consider a fully coupled reactive transport model. Instead, conservative transport is considered in both fractured and porous media and the reaction rates and precipitated mass is determined according to the methodology developed by De Simoni et al. (2007). For a simple bi-molecular reaction of two aqueous species A and B that are in equilibrium with a mineral AB ($AB = A + B$), the method by De Simoni allows to characterize the reactive transport problem completely in terms of the solution for conservative transport. The aqueous concentrations of A and B are expressed uniquely in terms of the concentration of the conservative species (De Simoni et al. 2007). The methodology is only valid in porous media.

The objectives of this test are (1) to prove the validity of the coupling of the reactive transport and fractures by comparing the flow and transport mass balance with the results from Martinez-Landa et al. (2012), (2) to compare the patterns of calcite precipitation, and (3) to investigate the sensitivity of the solution to the mass transfer term.

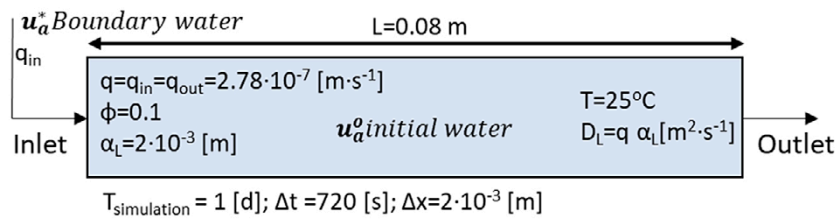


Figure 4-22. Schematic of benchmark setup and parameters.

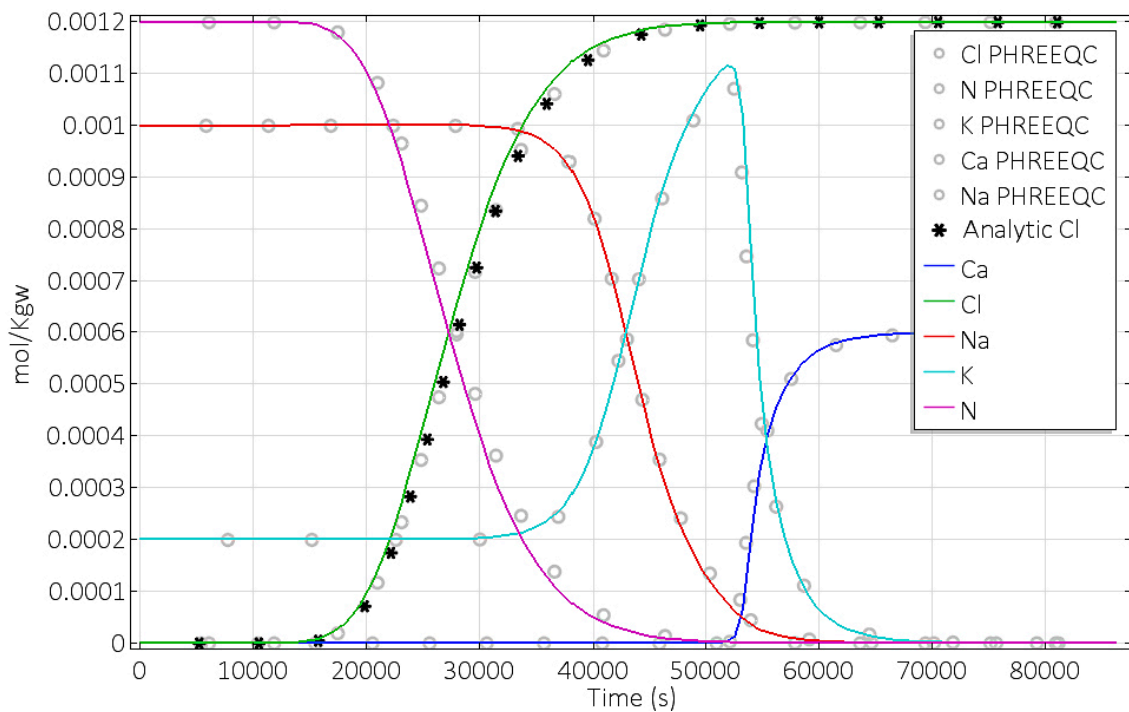


Figure 4-23. Comparison of breakthrough curves for PHREEQC (circles) and iCP (lines). Black points show the analytic solution of the ADE equation proposed by Ogata and Banks (1961).

Problem description

The model studies the behaviour of the chemical composition of the groundwater due to mixing between the natural water of the crystalline rock and water coming from a deep geological nuclear waste disposal facility. The model consists of a two-dimensional representation of a crystalline rock where the groundwater flow is controlled by fractures. The fractured medium is represented by a mixed discrete-continuum model. A square-shaped domain ($50 \times 50 \text{ m}^2$) of crystalline rock is intersected by three highly permeable fractures ($K = 5 \times 10^{-2} \text{ m/d}$). A smaller square-shaped domain of $5 \times 5 \text{ m}^2$ represents a nuclear waste repository (Figure 4-24). Table 4-5 contains the hydraulic and transport properties of the rock matrix, fractures and repository domain.

A steady-state groundwater flow field is simulated. Dirichlet boundary conditions are defined on the left and right boundaries to impose a unitary hydraulic gradient from left to right. The top and bottom boundaries are assumed as no-flow of both solute and water. Figure 4-24 shows the conceptual model from Martinez-Landa et al. (2012) and the computed water mass balance through the fractures (Fr-1 and Fr-2) and the matrix.

Table 4-5. Parameters used in the numerical simulations.

Parameter	Fracture	Crystalline rock	Repository
Conductivity (m/d) / Transmissivity (m^2/d)	5×10^{-2}	1×10^{-4}	1×10^{-3}
Aperture (m)	1	-	-
Porosity (-)	1×10^{-2}	3×10^{-3}	3×10^{-2}
Dispersivities (long/trans) (1/m)	0.4/0.3	0.4/0.3	0.4/0.3
Molecular diffusion (m^2/d)	8.64×10^{-5}	2.50×10^{-6}	2.50×10^{-6}

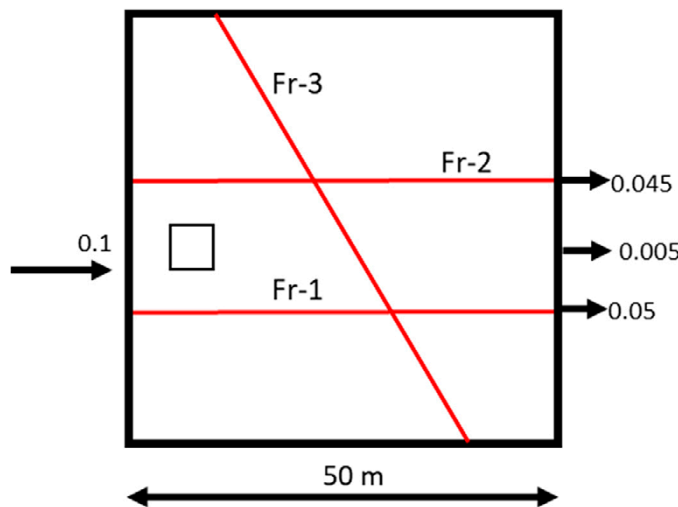


Figure 4-24. Water mass balance (m^3/day) reported in Martinez-Landa et al. (2012). Figure modified from Martinez-Landa et al. (2012).

The spatial discretization of the model is shown in Figure 4-25. The mesh has been refined around the matrix-fracture interface. The mesh has a total of 21 284 triangular finite elements (ECPM) and 747 edges (fracture domains).

The transport of a conservative tracer through the matrix and fractures is simulated for the ground-water flow in Figure 4-26. A tracer concentration equal to 1 mol/kg_w is initially present at the nuclear repository (small square-shaped domain in Figure 4-26). The background concentration in the rest of the domain is zero. The boundary conditions are inflow with a concentration equal to zero on the left boundary and outflow on the right boundary.

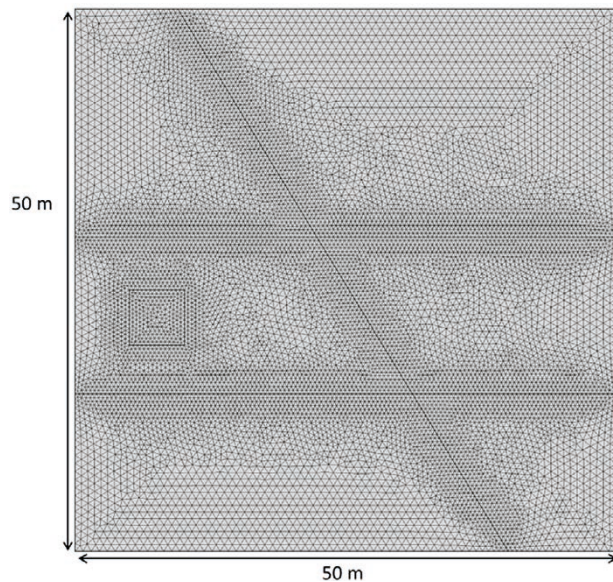


Figure 4-25. Finite element mesh for the reactive transport model.

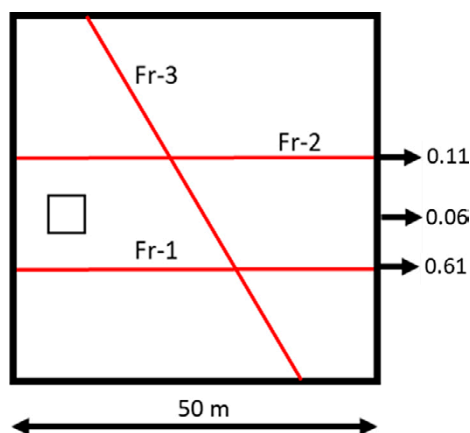


Figure 4-26. Global mass balance of the conservative tracer (-) in Martinez-Landa et al. (2012). The model considers an initial mass released of 0.78 (-). Figure modified from Martinez-Landa et al. (2012).

The accuracy of the coupling between the transport in the matrix and the fractures is evaluated through a comparison of the mass leaving the domain through the outlets of Fr-1, Fr-2 and the matrix (Figure 4-26). In addition, a sensitivity analysis to the value of β in the matrix-fracture exchange term (in Equation (3-18), Section 3.2.3) is carried out. The objectives of this sensitivity study are to test the validity range of the β parameter in a well characterized system, and to evaluate its effect on the mass exchange between the matrix and the fracture. In addition to that, a fully reactive transport model (RTM) is simulated with iCP under the previously calculated groundwater flow field. The RTM accounts for calcite precipitation promoted by the mixing between natural granitic water and water leached from concrete. The chemistry of the initial waters is shown in Table 4-6. The model accounts for calcite precipitation in the granitic matrix (ECPM) and in the three discrete fractures. The calcite dissolution/precipitation reaction is assumed to be in equilibrium (expression and equilibrium constant are shown in Table 4-7).

Table 4-6. Initial water composition and initial mineral amount.

	Granite/fracture	Repository
pH	8.1	13.37
Pe	12	11.541
Concentration (mol/kg_w)		
HCO ₃ ⁻	1.96 × 10 ⁻⁴	6.511 × 10 ⁻⁶
Ca	2.53 × 10 ⁻³	2.179 × 10 ⁻²
K	1.10 × 10 ⁻⁴	1.10 × 10 ⁻⁴
Mg	8.60 × 10 ⁻⁴	4.86 × 10 ⁻¹⁰
Na	6.00 × 10 ⁻⁴	6.0 × 10 ⁻³
Cl	6.99 × 10 ⁻³	6.99 × 10 ⁻³
Concentration (mol/dm³_{medium})		
Calcite	0	0

Table 4-7. Dissolution/precipitation reactions considered in the RTM.

Mineral	Formula	log K
Calcite	CaCO ₃ = +1.0 Ca ²⁺ -1.0 H ⁺ +1.0 HCO ₃ ⁻	1.84897

The results of the RTM are compared qualitatively with the results in Martinez-Landa et al. (2012). This comparison focuses on the precipitation patterns in the RTM solution and the patterns reported by Martinez-Landa et al. (2012). Their reported results show that most part of the mineral precipitates in the fracture at the top and farthest to the right. Larger amounts of precipitated calcite are observed in areas with high Darcy velocities and fracture intersections. These areas experience enhanced mixing between repository and the rock waters.

Results

The computed pressure field in steady state (Figure 4-27) shows a groundwater flow from left to right that is conditioned by the highly permeable fractures. Figure 4-28 shows the groundwater flow in the matrix (left) and in the 1D elements of the discrete fractures (right). The flow through the fractures is 20 times higher than through the matrix and most water leaves the domain through fractures Fr-1 and Fr-2. Table 4-8 shows the total outflow through the matrix and the fractures Fr-1 and Fr-2. The mass balance calculated in COMSOL is in good agreement with the one reported in Martinez-Landa et al. (2012). Small differences arise from the approximate geometry of the domains, which was obtained by measuring figures from the paper. This model serves as a good benchmark problem for the groundwater flow simulations using hybrid methods (porous media + discrete fracture networks).

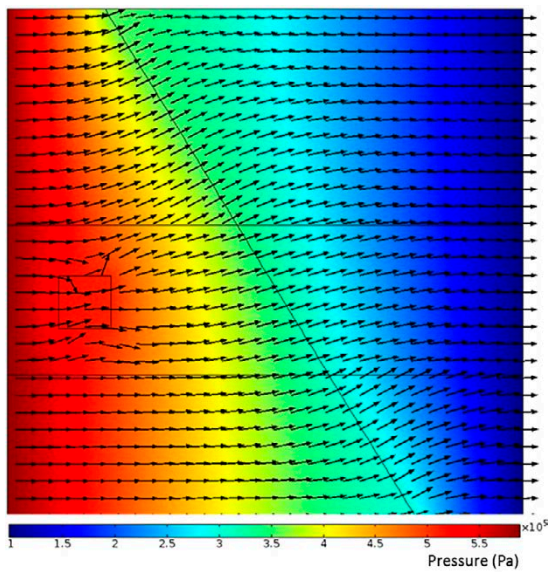


Figure 4-27. Calculated steady-state pressure field. Arrows illustrate the groundwater flow direction in the matrix (ECPM).

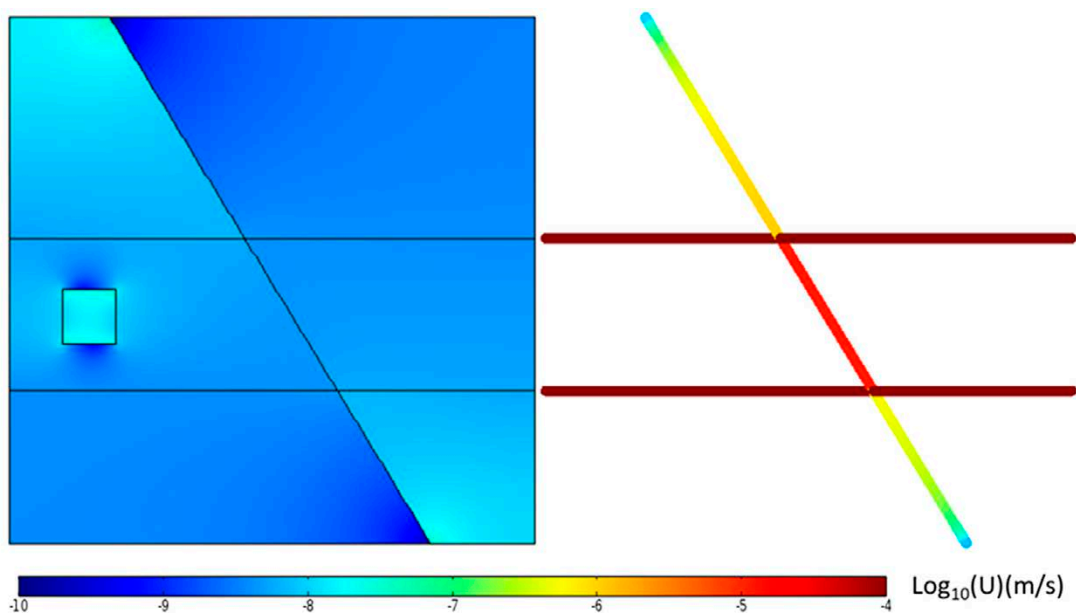


Figure 4-28. Magnitude of the Darcy velocity (in log scale) in the matrix (left) and the 1D fractures (right).

Table 4-8. Groundwater flow leaving the model through the different entities obtained in the COMSOL model and reported in Martinez-Landa et al. (2012).

	Matrix	Fr-1	Fr-2	Units
COMSOL	0.005	0.057	0.046	m^3/d
Reference	0.005	0.050	0.045	m^3/d

The transport of the conservative tracer released from the repository moving through the matrix and fractures is simulated. The initial concentration at the repository is 1 mol/kg_w. The tracer plume moves through the porous matrix and reaches fracture Fr-3 (Figure 4-29). There, the mixing of the matrix water with the larger flow through the fracture promotes a fast dilution of the tracer. This mixing is critical to capture in the reactive transport model as it induces calcite precipitation.

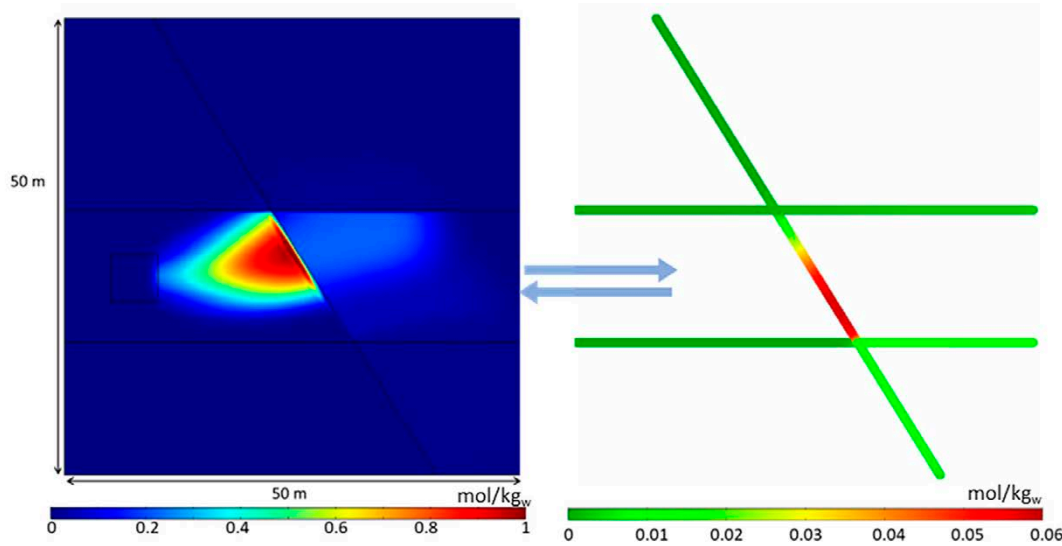


Figure 4-29. Concentration (mol/kg_w) of a conservative tracer released from the small square-shaped domain at 500 days of simulation in the matrix (left) and fracture (right).

The high flow velocities in the fractures reduce the residence times with respect to those in the matrix. Figure 4-30 shows the distribution of the tracer mass in time. The computed total mass is constant during the whole simulation reflecting the correct implementation of the two transport equations (Section 3.2.3). The tracer initially presented in the matrix reaches the fractures after 300 days. Since the storage of tracer in the fractures is very limited the tracer almost immediately reaches the fracture outlet at the right boundary. The accumulated mass outflow through each of the model outlets is also presented in Figure 4-30. 78 % of the total mass of tracer flows out of the domain through fracture Fr-1, 14 % leaves the domain through the fracture Fr-2 and the rest (8 %) through the matrix. Initially tracer leaves the system predominately via the fracture outlet of Fr-1, and later the tracer outflow via Fr-2 increases.

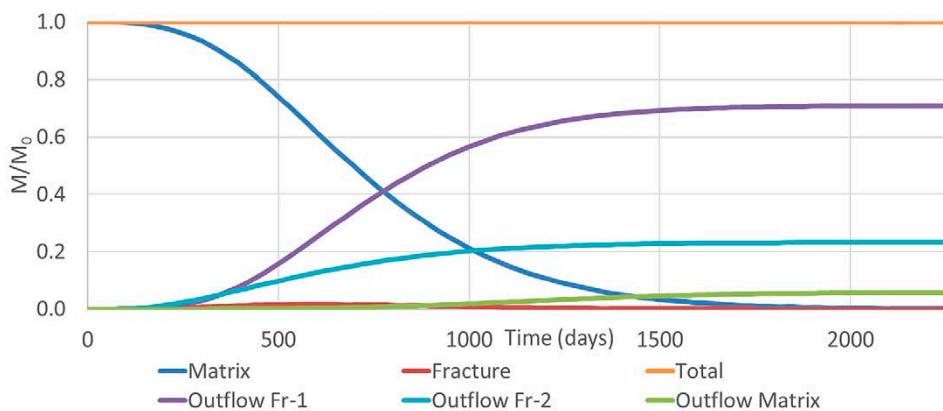


Figure 4-30. Temporal evolution of the distribution of tracer mass in the fractures and matrix domains over time and cumulative mass of tracer at the model outlets.

The considered problem is used to investigate the effect of the exchange term that couples the transport equations in the discrete fractures and the continuous matrix domain. A set of tracer transport simulations are performed varying the value of the β -parameter in the exchange term (Equation 3-18, Section 3.2.3). Here, the proportion of the mass outflow through the fractures and matrix outlets is used as a measurement of the exchange. Figure 4-31 shows the total mass leaving the domain for each outlet (Fr-1, Fr-2 and matrix) for different values of the parameter β . If this parameter is large enough, the coupled set of equations yield similar concentration values for the fracture and matrix. In that case, the mass exchange term (Equation 3-18), which has a form of a Cauchy boundary condition behaves as a Dirichlet-type boundary condition. Then, the mass exchange between the matrix and fracture does not depend on the value of β . However, if the value of β is lower than a given threshold, the exchange term behaves as a Neumann-type boundary condition. Then, the mass exchange between the two domains strongly depends on β and the tracer concentration at the matrix and at the fracture nodes are not equal, i.e., there is no concentration continuity at the fracture-matrix interface. The mass exchange is bounded between zero, when β is zero and the maximum mass exchange value, when β tends to infinity. For the problem presented here, the threshold value of β is 5×10^{-8} m/s (Figure 4-31). Values larger than that threshold yield a constant mass exchange between the matrix and the fractures. The mass balance (outflow) in those cases fits well the reference results by Martinez-Landa et al. (2012) (Figure 4-31). Notice that the mixed-discrete continuum method used in Martinez-Landa et al. (2012) imposes continuity in the matrix-fracture interface.

For this problem, not all the values of β are valid. β values lower than 8×10^{-10} m/s lead to a solution that does not conserve solute mass (Figure 4-31). From the hydrodynamic point of view, the fracture and the matrix are connected. The matrix is not completely impervious and there is flow from the matrix and the fracture. Therefore, using extremely low β values disconnect the solute transport from the matrix and the fracture and the flow and transport boundary conditions become inconsistent. In that case, β should be defined to include a contribution due to advection. As β has been defined as a diffusive flux, for this application, the range of validity of β values is restricted to values higher than 8×10^{-10} m/s. In summary, the definition of the β parameter used here is valid for transport in low permeable fractured media, in which the advection in the matrix is negligible. The validity of β values higher than a certain value is problem dependent. Thus, simulation cases where advection in matrix is relevant will require of a dedicated study to test the range of β where the mass is conserved.

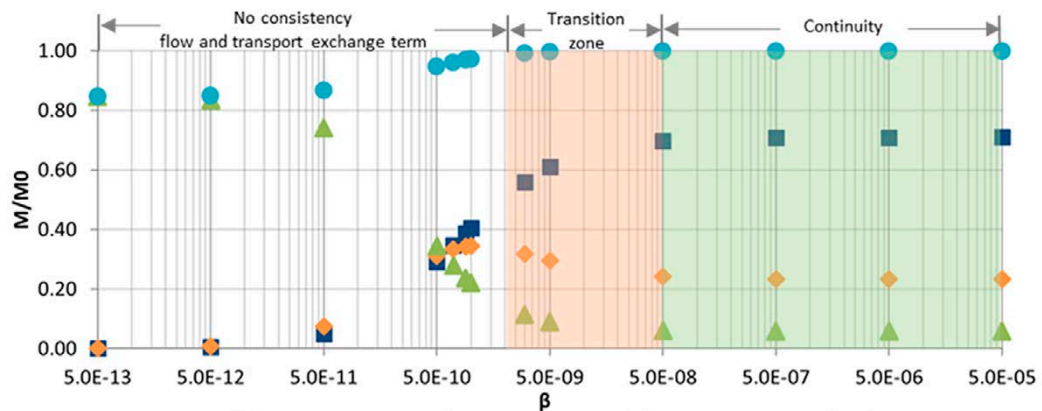


Figure 4-31. Normalized total tracer mass through the model outlets for different values of β .

In addition to the conservative tracer transport problem, a reactive transport problem is solved in the same groundwater flow field. Two initial waters are considered: one is a resident CO_3^{2-} -rich granitic water and the other is a calcium-rich water leached from concrete in the repository. Both waters are undersaturated with respect to calcite. However, when they mix the resulting water becomes oversaturated with respect to calcite. Figure 4-32 shows the saturation index of the calcite for different mixing ratios between these two initial waters (Table 4-6). Mixing ratios of granitic waters higher than 0.65 lead to calcite precipitation.

The results show the advection and dispersion of a plume of calcium moving from the repository through the porous matrix to the right before reaching the fractures (Figure 4-33). The calcium concentration in the fracture is lower than the one in the matrix. This is because of dilution by the relatively high water flow in the fracture (Figure 4-28) and precipitation of calcite (CaCO_3). Calcite precipitation, driven by mixing, occurs at the interface between the calcium plume and the granitic water. Calcite precipitates upstream of the repository, where water leached from concrete diffuses into the flowing granitic water. Downstream of the repository, calcite precipitates in the fracture intersections, where mixing is enhanced, and in the adjacent matrix. The calcite precipitation zones resemble those reported in Martinez-Landa et al. (2012).

The precipitation occurs in areas where the two waters mix (Figure 4-34). The temporal evolution of the calcite precipitation in the matrix and fractured domain is presented in Figure 4-35. Most calcite precipitates along the discrete fractures as quantified by Martinez-Landa et al. (2012) due to the enhance mixing caused by the large water flows. However, after the Ca-rich plume leaves the system the continuous flushing of the system with unsaturated granitic water causes redissolution of some of the calcite (Figure 4-35). Maximum calcite precipitation is observed after 1 500 days and monotonically decreases afterwards. This result differs from Martinez-Landa et al. (2012), because they considered calcite precipitation as an irreversible reaction.

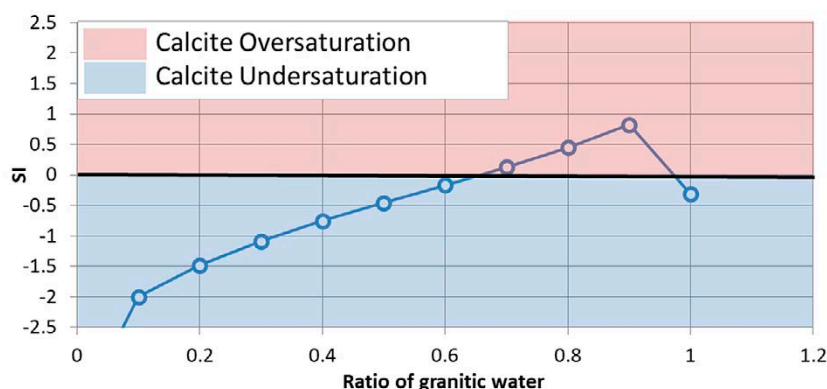


Figure 4-32. Calcite saturation index for different mixing ratios of the two waters. The calculations have been performed in PHREEQC.

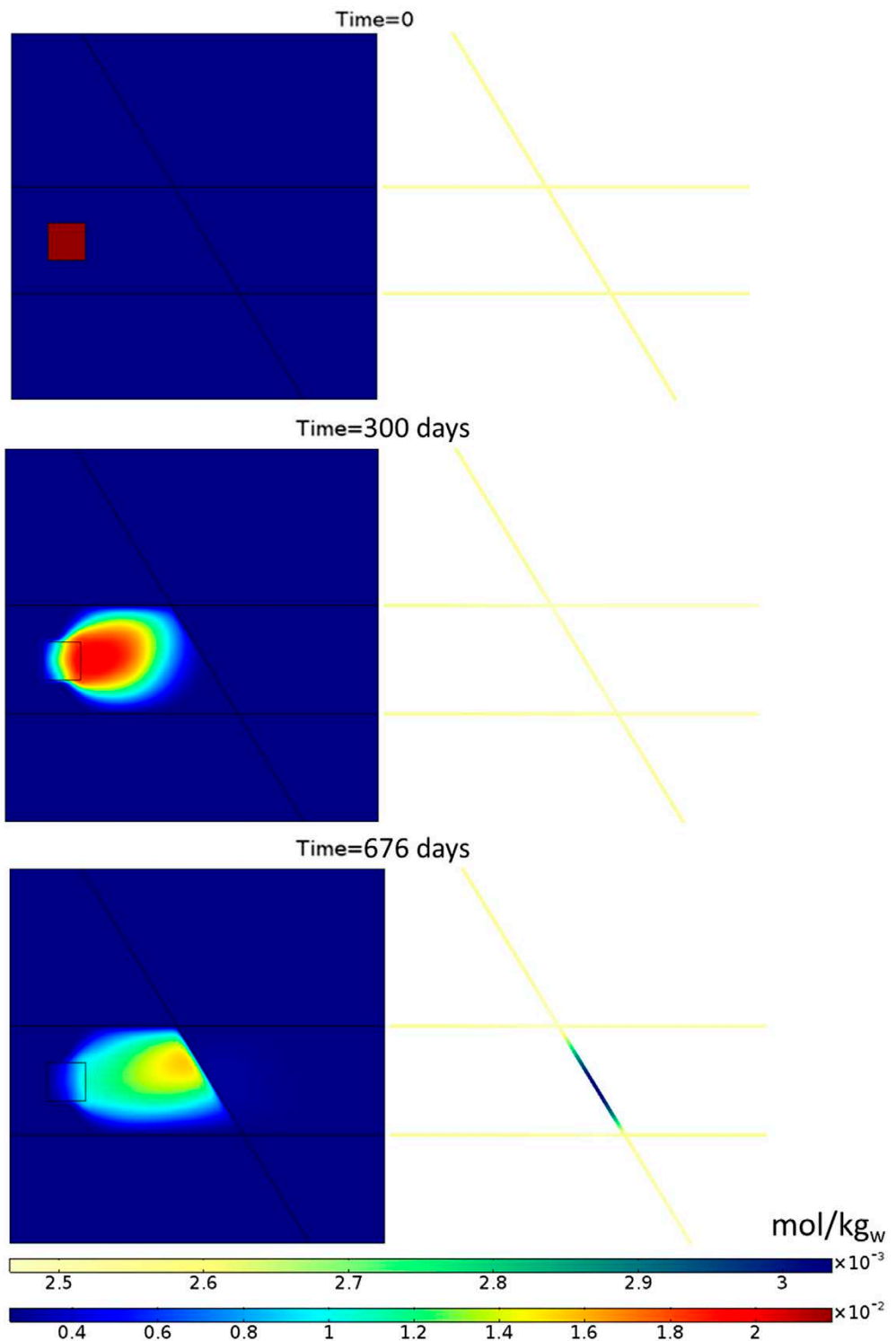


Figure 4-33. Calcium concentration in the matrix (left) and in the fractures (right) at different times.

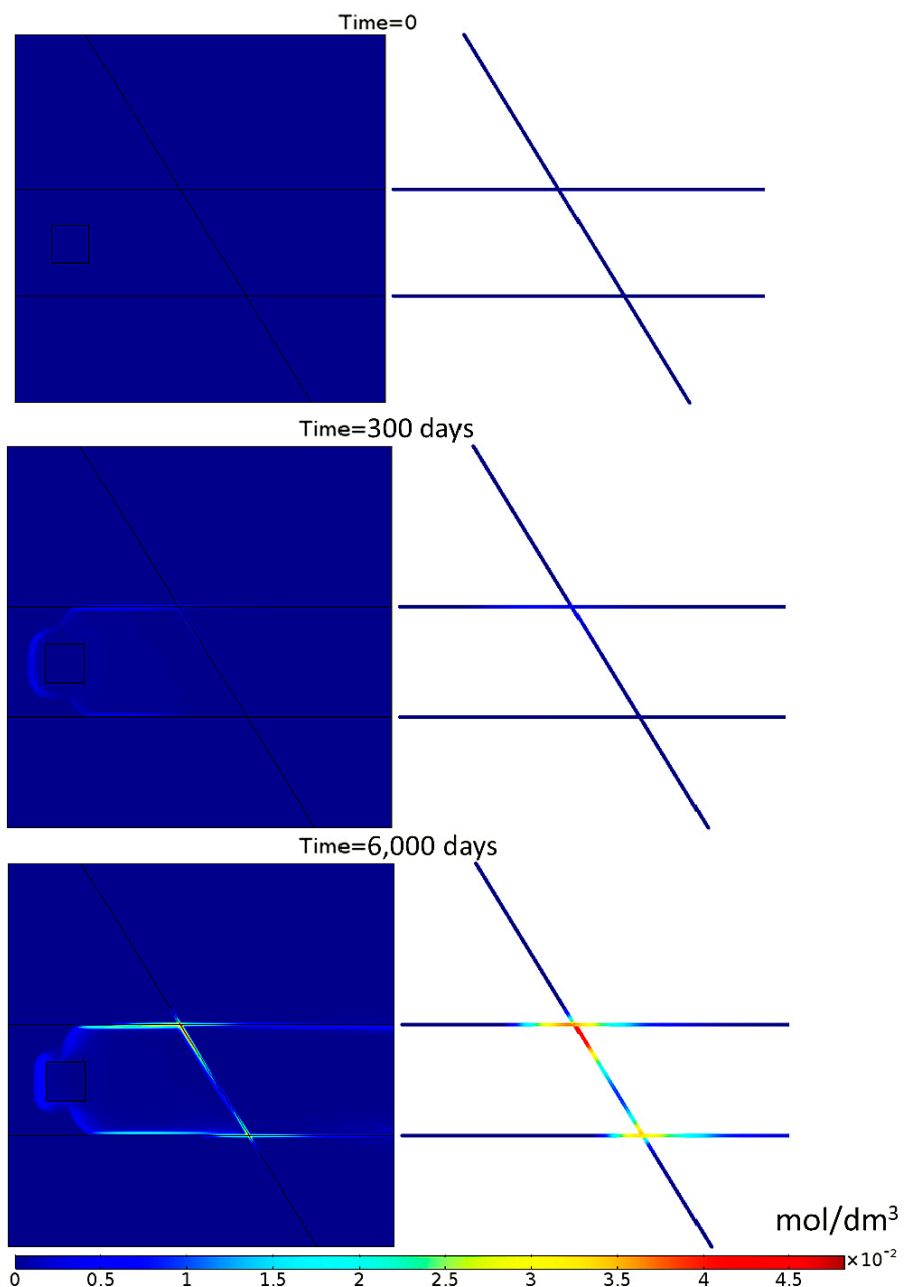


Figure 4-34. Calcite mineral distribution in the matrix (left) and fracture (right) at different times.

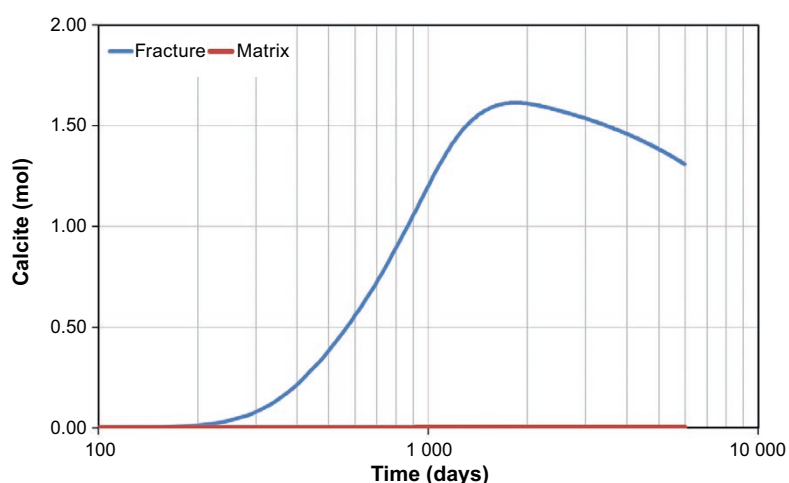


Figure 4-35. Calcite precipitation in the matrix and fractures over time.

5 Conclusions

This report presents a tool for reactive transport modelling in hybrid systems composed of a reactive porous matrix and reactive discrete fractures. The tool is an extension of the interface COMSOL-PHREEQC, iCP (Nardi et al. 2014).

The groundwater flow and transport in the fractured media are modelled using COMSOL Multiphysics. During the development of the tool, it was necessary to carry out a thorough analysis of its capability to model discrete fractures and hybrid continuum-discrete systems. Therefore, a set of benchmark problems for flow and transport in fractured systems were solved using COMSOL Multiphysics.

A set of four benchmark problems for groundwater flow in fractured media (taken from Flemisch et al. 2018) was simulated. The problems are of different complexity, ranging from a simplified geometry with two fractures to a case based on data from an actual outcrop located in Norway. Numerical results demonstrate that COMSOL reproduces all of the previously reported solutions. Thus, the COMSOL simulations reproduce properly the impact of fractures that cross the entire domain and fractures embedded in a porous medium. The default method to solve flow in fractures in COMSOL assumes pressure continuity at the interface between a porous medium and a discrete fracture. Therefore, the method is suitable only for high permeability fractures that act as preferential pathways. This is the case of fractured crystalline rocks where flow is controlled by permeable fractures. The representation of low permeability fractures that act as flow barriers is a challenge for many groundwater flow codes. The numerical method must be able to represent a pressure discontinuity caused by the low permeability fractures. In COMSOL, a boundary condition called “Thin barriers” can be used at the low permeability barriers. This boundary condition allows to capture pressure jumps between the matrix at both sides of the fracture. When this boundary condition is applied, COMSOL correctly reproduces the benchmark problems for low permeability fractures as well.

The benchmarking of the conservative transport was carried out by comparing the results obtained using only COMSOL and also using iCP against the analytical solution proposed by Tang et al. (1981) and the results of a synthetic 2D mixed discrete-continuum problem reported in Martinez-Landa et al. (2012). In both cases there is a good agreement between the COMSOL results and the reported solutions. The transport problem presented by Tang et al. (1981) was solved numerically using different representations of the fractures (Figure 4-19). The results show that the different representations of the fractured media generate similar results although the computational burden is different. The most efficient method is the approach where the matrix is represented as an extra dimension. This method will be useful for complex fracture network configurations where the matrix domain is difficult to mesh.

The development of the reactive transport tool for fractured media was carried out following a stepwise methodology of increasing complexity. First, a problem of reactive transport in a discrete fracture is solved, in which the discrete fracture is modelled and the interaction with the matrix is neglected. Secondly, the transport in discrete fractures embedded in porous media (hybrid method) is considered. Both the matrix and the discrete fractures are considered to be reactive. As a result, iCP has been modified to solve reactive transport model in pure DFN and also in hybrid models with reactive fractures. Two benchmark problems are proposed and solved. The extension of iCP is shown to be able to handle reactive transport in low permeable fractured media, in which the advection in the matrix is negligible. The results serve to validate the technical developments and remark the high potential of iCP as an RTM tool to couple several physical and chemical processes.

The methodology to perform reactive simulations in fractured media presented in this report is limited to systems where fractures are more permeable than the porous matrix. Simulations where the fractures act as barriers for flow and transport can be performed using the “thin barrier” boundary condition but in this case the fracture will not be reactive. The new development here presented does not add any limitation in terms of simulation times and computer requirements to the ones already existing for COMSOL and iCP. Thus, the main limitation of iCP is the large RAM memory required and the large computation times for large models with a large number of elements.

References

SKB's (Svensk Kärnbränslehantering AB) publications can be found at www.skb.com/publications.

- Applegate D, Appleyard P, Joyce S, 2020.** Modelling solute transport and water–rock interactions in discrete fracture networks. Posiva Working Report 2020-01, Posiva Oy, Finland.
- Barry D A, Miller C T, Culligan-Hensley P J, 1996.** Temporal discretization errors in non-iterative split-operator approaches to solving chemical reaction/groundwater transport models. *Journal of Contaminant Hydrology* 22, 1–17.
- Baxter S, Hartley L, Hoek J, Myers S, Tsitsopoulos V, Williams T, 2019.** Upscaling of brittle deformation zone flow and transport properties. SKB R-19-01, Svensk Kärnbränslehantering AB.
- Bazrafkan S, Matthai S K, Mindel J E, 2014.** The Finite-element-centered Finite-volume Discretization Method (FECFVM) for multiphase transport in porous media with sharp material discontinuities. In Proceedings of ECMOR XIV – 14th European Conference on the Mathematics of Oil Recovery. European Association of Geoscientists & Engineers, 1–22. <https://doi.org/10.3997/2214-4609.20141841>
- Bear J, 1972.** Dynamics of fluids in porous media. New York: Elsevier.
- Berkowitz B, 2002.** Characterizing flow and transport in fractured geological media: A review. *Advances in Water Resources* 25, 861–884.
- Berkowitz B, Scher H, 1997.** Anomalous transport in random fracture networks. *Physical Review Letters* 79, 4038–4041.
- Berkowitz B, Scher H, 1998.** Theory of anomalous chemical transport in random fracture networks. *Physical Review E* 57, 5858–5869.
- Carrera J, Galarza G, Medina A, Vives L, 1995.** Transin: Modelos de flujo y transporte con simulación de fracturas. ENRESA 10, 48–49. (In Spanish.)
- Carrera J, Sánchez-Vila X, Benet I, Medina A, Galarza G, Guimerà J, 1998.** On matrix diffusion: formulations, solution methods and qualitative effects. *Hydrogeology Journal* 6, 178–190.
- Charlton S R, Parkhurst D L, 2011.** Modules based on the geochemical model PHREEQC for use in scripting and programming languages. *Computers & Geosciences* 37, 1653–1663. <https://doi.org/10.1016/j.cageo.2011.02.005>
- COMSOL, 2017.** COMSOL Multiphysics. Reference guide, version 5.3. Burlington, MA: COMSOL Inc.
- D'Angelo C, Scotti A, 2012.** A mixed finite element method for Darcy flow in fractured porous media with non-matching grids. *ESAIM: Mathematical Modelling and Numerical Analysis* 46, 465–489.
- Darcy H, 1856.** Les fontaines publiques de la ville de Dijon: exposition et application des principes à suivre et des formules à employer dans les questions de distribution d'eau: ouvrage terminé par un appendice relatif aux fournitures d'eau de plusieurs villes au filtrage des eaux et à la fabrication des tuyaux de fonte, de plomb, de toile et de bitume. Paris: Dalmont. (In French.)
- Dentz M, Berkowitz B, 2003.** Transport behaviour of a passive solute in continuous time random walks and multirate mass transfer. *Water Resources Research* 39. doi:10.1029/2001WR001163
- De Simoni M, Sanchez-Vila X, Carrera J, Saaltink M, 2007.** A mixing ratios-based formulation for multicomponent reactive transport. *Water Resources Research* 43. doi:10.1029/2006WR005256
- Diersch H J, 2013.** FEFLOW: finite element modeling of flow, mass and heat transport in porous and fractured media. Berlin: Springer.
- Dietrich P, Helmig R, Sauter M, Hötzl H, Köngeter J, Teutsch G (eds), 2005.** Flow and transport in fractured porous media. Berlin: Springer.
- Flemisch B, Berre I, Boon W, Fumagalli A, Schwenck N, Scotti A, Stefansson I, Tatomir A, 2018.** Benchmarks for single-phase flow in fractured porous media. *Advances in Water Resources* 111, 239–258.

- Ford N T, Silverton T R, Cottrell M G, 2008.** Rock mass characterisation of a prospective base metal deposit using a combined FracMan/ELFEN approach. In Potvin Y, Carter J, Dyskin A, Jeffrey R (eds). SHIRMS 2008: Proceedings of the First Southern Hemisphere International Rock Mechanics Symposium, Perth. Australian Centre for Geomechanics, 605–617.
- Frith N, Martin V, Roberts J E, Saâda A, 2012.** Modelling fractures as interfaces with nonmatching grids. Computational Geosciences 16, 1043–1060.
- Geiger S, Dentz M, Neuweiler I, 2013.** A novel multi-rate dual-porosity model for improved simulation of fractured and multi-porosity reservoirs. SPE Journal 18, 670–684.
- Gelhar L W, Axness C L, 1983.** Three-dimensional stochastic analysis of macrodispersion in aquifers. Water Resources Research 19, 161–180.
- Gelhar L W, Welty C, Rehfeldt K R, 1992.** A critical review of data on field-scale dispersion in aquifers. Water Resources Research 28, 1955–1974.
- Grisak G E, Pickens J F, 1980.** Solute transport through fractured media: 1. The effect of matrix diffusion. Water Resources Research 16, 719–730.
- Hadgu T, Karra S, Kalinina E, Makedonska N, Hyman J D, Klise K, Viswanathan H S, Wang Y, 2017.** A comparative study of discrete fracture network and equivalent continuum models for simulating flow and transport in the far field of a hypothetical nuclear waste repository in crystalline host rock. Journal of Hydrology 553, 59–70.
- Haggerty R, Gorelik S M, 1995.** Multiple-rate mass transfer for modeling diffusion and surface reactions in media with pore-scale heterogeneity. Water Resources Research 31, 2383–2400.
- Hajibeygi H, Karvounis D, Jenny P, 2011.** A hierarchical fracture model for the iterative multiscale finite volume method. Journal of Computational Physics 230, 8729–8743.
- Hammond G, Lichtner P, Lu C, 2007.** Subsurface multiphase flow and multicomponent reactive transport modeling using high-performance computing. Journal of Physics: Conference Series 78, 012025. doi:10.1088/1742-6596/78/1/012025
- Hammond G E, Lichtner P C, 2010.** Field-scale model for the natural attenuation of uranium at the Hanford 300 Area using high-performance computing. Water Resources Research 46. doi:10.1029/2009WR008819
- Harbaugh A W, 2005.** MODFLOW-2005: the U.S. Geological Survey modular ground-water model – the ground-water flow process. Techniques and Methods 6-A16, U.S. Geological Survey.
- Harris A W, Atkinson A, Balek V, Brodersen K, Cole G B, Haworth A, Malek Z, Nickerson A K, Nilsson K, Smith A C, 1997.** The performance of cementitious barriers in repositories. Final report. EUR 17643, European Commission.
- Hartley L J, Herbert A W, Wilcock P M, 1996.** NAPSAC (release 4.0) summary document. Report AEA-D&R-0271, AEA Technology.
- Helming R, 1997.** Multiphase flow and transport processes in the subsurface: a contribution to the modelling of hydroystems. Berlin: Springer.
- Hollenbeck K J, Harvey C F, Haggerty R, Werth C J, 1999.** A method for estimating distributions of mass transfer rate coefficients with applications to purge and batch experiments. Journal of Contaminant Hydrology 37, 367–388.
- Hoteit H, Firoozabadi A, 2008.** Numerical modeling of two-phase flow in heterogeneous permeable media with different capillarity pressures. Advances in Water Resources 31, 56–73.
- Huang H, Long T A, Wan J, Brown W P, 2011.** On the use of enriched finite element method to model subsurface features in porous media flow problems. Computational Geosciences 15, 721–736.
- Hyman J D, Karra S, Makedonska N, Gable C W, Painter S L, Viswanathan H S, 2015.** DFNWORKS: A discrete fracture network framework for modeling subsurface flow and transport. Computers & Geosciences 84, 10–19.
- Iraola A, Trinchero P, Karra S, Molinero J, 2019.** Assessing dual continuum method for multi-component reactive transport. Computers & Geosciences 130, 11–19.

- Jackson C P, Hoch A R, Todman S, 2000.** Self-consistency of a heterogeneous continuum porous medium representation of a fractured medium. *Water Resources Research* 36, 189–202.
- Jacobs, 2021.** ConnectFlow Technical summary, Version 12.3. Didcot, UK: Jacobs.
- Karim-Fard M, Durlofsky L J, Aziz K, 2004.** An efficient discrete-fracture model applicable for general purpose reservoir simulators. *SPE Journal* 9, 227–236.
- Karimzadeh L, Lippmann-Pipke J, Franke K, Lippold H, 2017.** Mobility and transport of copper (II) influenced by the microbial siderophore DFOB: Column experiment and modelling. *Chemosphere* 173, 326–329.
- Kolditz O, Görke U-J, Shao H, Wang W (eds), 2012.** Thermo-hydro-mechanical-chemical processes in porous media: benchmarks and examples. Berlin: Springer.
- Lei Q, Lathan J-P, Tsang C-F, 2017.** The use of discrete fracture networks for modelling coupled geomechanical and hydrological behaviour of fractured rocks. *Computers and Geotechnics* 85, 151–176.
- Martin V, Jaffré J, Roberts J E, 2005.** Modelling fractures and barriers as interfaces for flow in porous media. *SIAM Journal on Scientific Computing* 26, 1667–1691.
- Martinez-Landa L, Carrera J, Dentz M, Fernández-García D, Nardí A, Saaltink M W, 2012.** Mixing induced reactive transport in fractured crystalline rocks. *Applied Geochemistry* 27, 479–489.
- Milliotte C, Jonoud S, Wennberg O P, Matthäi S K, Jurkiw A, Mosser L, 2018.** Well-data-based discrete fracture and matrix modelling and flow-based upscaling of multilayer carbonate reservoir horizons. Geological Society, London, Special Publications 459, 191–210.
- Moinfar A, Narr W, Hui M-H, Mallison B, Lee S H, 2011.** Comparison of discrete-fracture and dual-permeability models for multiphase flow in naturally fractured reservoirs. SPE Reservoir Simulation Symposium, The Woodlands, Texas, February 2011. Society of Petroleum Engineers. doi:10.2118/142295-MS
- Monteagudo J E P, Firoozabadi A, 2004.** Control volume method for numerical simulation of two phase immiscible flow in two and three-dimensional discrete fractured media. *Water Resources Research* 40. doi:10.1029/2003WR002996
- Nardi A, Idiart A, Trinchero P, de Vries L M, Molinero J, 2014.** Interface COMSOL-PHREEQC (iCP), an efficient numerical framework for the solution of coupled Multiphysics and geochemistry. *Computers & Geosciences* 69, 10–21.
- Nardi A, Sáinz-García A, de Vries L M, Negro D, Coene E, Bayer M, Trinchero P, Idiart A, Pekala M, Abarca E, Silva O, Molinero J, 2020.** Interface COMSOL-PHREEQC (iCP), User's guide, version 1.6.0. Available at: <https://gitlab.amphos21.com/public-projects/icp-documentation/>
- Neretnieks I, 1980.** Transport mechanisms and rates of transport of radionuclides in the geosphere as related to the Swedish KBS concept. In *Underground disposal of radioactive wastes: proceedings of a symposium on the underground disposal of radioactive wastes*, Otaniemi, Finland, 2–6 July 1979. Vol 2. Paris: OECD Nuclear Energy Agency, 315–338.
- Neuman S P, 2005.** Trends, prospects and challenges in quantifying flow and transport through fractured rocks. *Hydrogeology Journal* 13, 124–147.
- Nick H M, Matthäi S K, 2011.** A hybrid finite-element finite-volume method with embedded discontinuities for solute transport in heterogeneous media. *Vadose Zone Journal* 10, 299–312.
- Odsæter L H, Kvamsdal T, Larson M G, 2019.** A simple embedded discrete fracture-matrix model for a coupled flow and transport problem in porous media. *Computer Methods in Applied Mechanics and Engineering* 343, 572–601. <https://doi.org/10.1016/j.cma.2018.09.003>
- OECD, 1987.** The international HYDROCOIN project: background and results. Paris: OECD Nuclear Energy Agency.
- Ogata A, Banks R B, 1961.** A solution of the differential equation of longitudinal dispersion in porous media. Fluid movement in earth materials. Geological Survey Professional Paper 411-A. Washington: U.S. Government Printing Office.

- Painter S, Cvetkovic V, 2005.** Upscaling discrete fracture network simulations: An alternative to continuum transport models. *Water Resources Research* 41. doi:10.1029/2004WR003682
- Parkhurst D L, Appelo C, 2013.** Description of input and examples for PHREEQC version 3: a computer program for speciation, batch-reaction, one-dimensional transport, and inverse geochemical calculations. U.S. Geological Survey. <https://pubs.usgs.gov/tm/06/a43/>
- Parkhurst D L, Kipp K L, Engesgaard P, Charlton S R, 2004.** PHAST – A program for simulating ground-water flow, solute transport, and multicomponent geochemical reactions. U.S. Department of the Interior, U.S. Geological Survey. <https://pubs.usgs.gov/tm/2005/tm6A8/>
- Prommer H, Davis G B, Barry D A, 1999.** PHT3D – a three-dimensional biogeochemical transport model for modelling natural and enhanced remediation. In Johnston C D (ed). *Proceedings of the Contaminated Site Remediation Conference: Challenges Posed by Urban and Industrial Contaminants*, Fremantle, Western Australia. Wembley: Centre for Groundwater Studies, CSIRO, 351–358.
- Reichenberger V, Jakobs H, Bastian P, Helmig R, 2006.** A mixed-dimensional finite volume method for two-phase flow in fractured porous media. *Advances in Water Resources* 29, 1020–1036.
- Remy N, Boucher A, Wu J, 2009.** Applied geostatistics with SGeMS: a user's guide. Cambridge: Cambridge University Press.
- Renard P, de Marsily G, 1997.** Calculating equivalent permeability: a review. *Advances in Water Resources* 20, 253–278.
- Saaltink M, Benet I, Ayora C, 1997.** RETRASO, Fortran code for solving 2D reactive transport of solutes, users' guide. Departamento de Ingeniería del Terreno, Universitat Politècnica de Catalunya and Instituto de Ciencias de la Tierra, CSIC, Barcelona.
- Saaltink M W, Ayora C, Carrera J, 1998.** A mathematical formulation for reactive transport that eliminates mineral concentration. *Water Resources Research* 34, 1649–1656.
- Sahimi M, 2011.** Flow and transport in porous media and fractured rock: from classical methods to modern approaches. Hoboken, NJ: Wiley.
- Sainz-Garcia A, Abarca E, Nardi A, Grandia F, Oelkers E H, 2017.** Convective mixing fingers and chemistry interaction in carbon storage. *International Journal of Greenhouse Gas Control* 58, 52–61.
- Sampietro D, Pool M, Abarca E, Molinero J, 2022.** iCP version 2.0: A numerical tool for solving reactive transport in discrete fractures with matrix diffusion. SKB R-21-10, Svensk Kärnbränslehantering AB.
- Schwenck N, 2015.** An XFEM-based model for fluid flow in fractured porous media. PhD thesis. University of Stuttgart, Department of Hydromechanics and Modelling of Hydrosystems.
- Sidborn M, Marsic N, Crawford J, Joyce S, Hartley L, Idiart A, de Vries L M, Maia F, Molinero J, Svensson U, Vidstrand P, Alexander R, 2014.** Potential alkaline conditions for deposition holes of a repository in Forsmark as a consequence of OPC grouting. Revised final report after review. SKB R-12-17, Svensk Kärnbränslehantering AB.
- Šimůnek J, Jacques D, van Genuchten M T, Mallants D, 2006.** Multicomponent geochemical transport modelling using HYDRUS-1D and HP1. *Journal of the American Water Resources Association* 42, 1537–1547.
- Singhal B B S, Gupta R P, 2010.** Applied hydrogeology of fractured rocks. 2nd ed. Dordrecht: Springer.
- Smith W R, Missen R W, 1982.** Chemical reaction equilibrium analysis: theory and algorithms. New York: Wiley.
- Steefel C I, MacQuarrie K T B, 1996.** Approaches to modelling reactive transport in porous media. In Lichtner P C, Steefel C I, Oelkers E H (eds). *Reactive Transport in Porous Media*. Washington, DC: Mineralogical Society of America, 83–125.
- Steefel C I, DePaolo D J, Lichtner P C, 2005.** Reactive transport modeling: An essential tool and a new research approach for the Earth sciences. *Earth and Planetary Science Letters* 240, 539–558.

- Strang G, 1968.** On the construction and comparison of difference schemes. SIAM Journal on Numerical Analysis 5, 506–517.
- Svensson U, 2001.** A continuum representation of fracture networks. Part I: Method and basic test cases. Journal of Hydrology 250, 170–186.
- Svensson U, Ferry M, 2010.** Darcy Tools version 3.4. User's guide. SKB R-10-72, Svensk Kärnbränslehantering AB.
- Tang D H, Frind E O, Sudicky E A, 1981.** Contaminant transport in fractured porous media: analytical solution for a single fracture. Water Resources Research 17, 555–564.

SKB is responsible for managing spent nuclear fuel and radioactive waste produced by the Swedish nuclear power plants such that man and the environment are protected in the near and distant future.

skb.se